AD-A036 611 MAGNAVOX RESEARCH LABS TORRANCE CALIF F/G 15/1
SIGNAL PROCESSING APPLICATIONS OF MAGNETO-OPTIC THIN FILMS,(U)
JAN 68 R E ESCHELBACH
UNCLASSIFIED MX-TR-8-690-2005-68 NL

| OF |
ADA036611

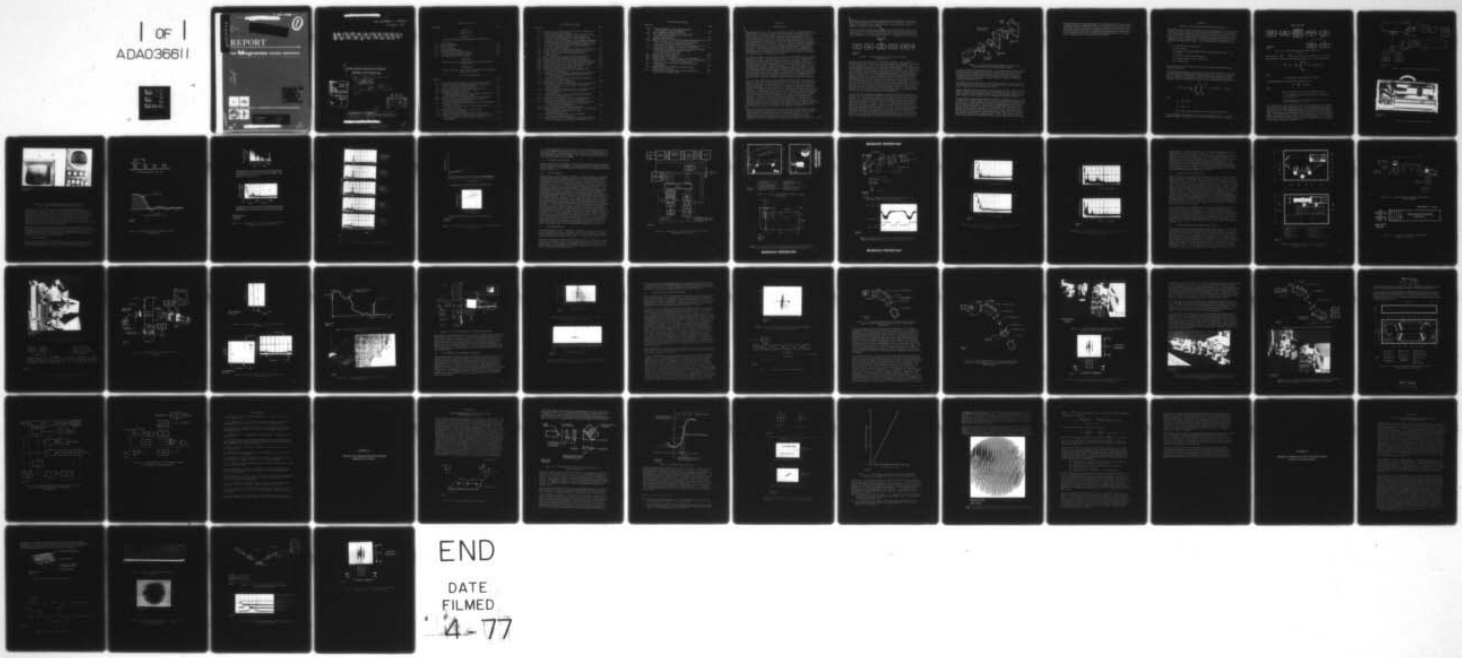

END

DATE
FILMED
4-77

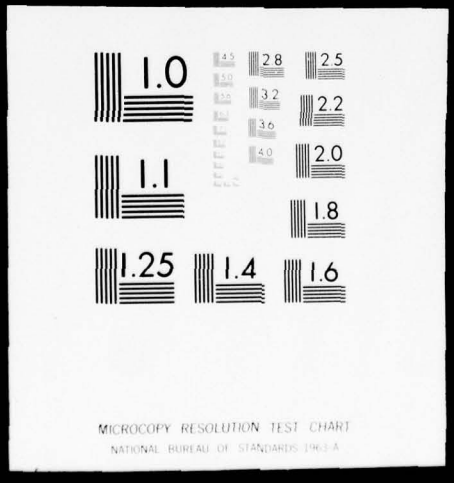

MOST Project 1-3

[redacted]

REPORT

FROM··· **Magnavox** RESEARCH LABORATORIES

TORRANCE • CALIFORNIA

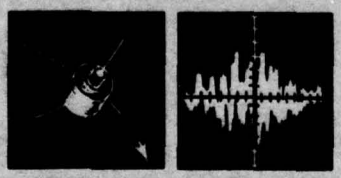

THE MAGNAVOX COMPANY··· GOVERNMENT AND INDUSTRIAL DIVISION

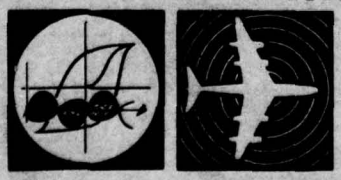

[redacted]

[redacted]

(1)

MPI CONTROL # 034 A

COPY 16 OF 120 COPIES

(6)

SIGNAL PROCESSING APPLICATIONS OF MAGNETO-OPTIC THIN FILMS

by

(10) R. E. Eschelbach

January 1968

Reprinted June 1968

(11) Jan 68 (12) 59 p.

(14)

DISTRIBUTION STATEMENT A
Approved for public release;
Distribution Unlimited

MX-TR-8-690-2005-68

[redacted]

214410

TABLE OF CONTENTS

LIST OF ILLUSTRATIONS

ILLUSTRATIONS (Contd)

ILLUSTRATIONS (Contd)

SECTION 1

INTRODUCTION

During the past few years, radar, communication and sonar system performance requirements have increased to a point where it is necessary to store and process a far greater number of electrical signals, in as near real time as possible, than ever before. Integrated microelectronic circuits (IC's) have alleviated some of the less stringent processing requirements by providing storage capacities of a few hundred or a few thousand bits at MHz rates, thus allowing sophisticated time compression processing of the stored information. However, current processing needs with larger storage requirements can be met only with bulky equipment involving the inefficient use of core or film storage, and are not suitable for installation in compact mobile processors. While large scale integration (LSI) promises to allow sophisticated processing of several hundred bits in reasonable volumes, the requirement for compact equipment for the rapid processing of thousands of bits at high rates is difficult to meet at this time by strictly electronic means.

The inherent benefits in the use of optics versus conventional electronics for processing electrical signals is well documented (reference 1, 2, 3 and 4). The advantages stem from the Fourier transform properties of optical lenses and the ability of cylindrical lenses to handle many parallel channels with reasonable-sized optics. The problems encountered in the optical processing of electrical signals center mainly on the limitations of available spatial light modulators. A standard technique for converting electrical signals to images is to photograph the line scan output of a cathode ray tube display that is intensity modulated with the desired signal. In this case the film serves as the spatial light modulator. This approach, while giving both a large time bandwidth product and a multichannel capability, has the disadvantage of requiring a time delay to process the film before the signals can be processed. While this delay can be minimized, the bulk of equipment required can also be undesirable.

Other currently available real-time spatial light modulators tend to employ acoustic delay lines, thermally variable plastics, photochromic materials, electrostatically deflected membranes, electrolytic materials, etc.; and make use of the Sears-Debye effect or appropriate electron or light beams to modulate the light beam incident on the delay line, plastic or chemical medium, by changes in transmisivity, reflectance, phase or a combination of these effects. Each light modulator technique has its own peculiar set of constraints. In the delay line case, the modulator has a large bandwidth but is limited on the available time aperture by the velocity of sound in the material. Thus, even a fraction of a second integration time would require unrealistic optical apertures. The thermal-plastic case removes this problem but requires bulky modulators to produce a reasonable time-bandwidth product. Photochromic modulators are improving, but are not yet at a state of development to be considered for field applications because of the light intensity required for proper exposure. Membrane and other addressed element modulators, while offering moderate density and bandwidth, require the storage of the signals be external to the modulator itself.

Large time bandwidth products under a limited bandwidth constraint demand optical apertures which tend to dissipate the savings in cost and volume of optical processing over electronic processing with currently available light modulators. However, a unique solution to this problem has been demonstrated at Magnavox Research Laboratories based on the magneto-optic properties of ferromagnetic thin film materials. This approach constitutes a technical breakthrough, since it offers the

OVER

advantage of packing several hundred thousand to several million bits to the square inch of modulator surface at rates varying from DC to several MHz. This allows large time bandwidth products, multiple channels, and small optical apertures, resulting in a small processing volume.

Before covering the specific areas of application that are the subject of this report, a brief review of the components and properties of an analog optical signal processer will be introduced. To this end, consider the basic components of a simple analog optical signal processer as illustrated in Figure 1-1. An input electrical signal $E_i(t)$

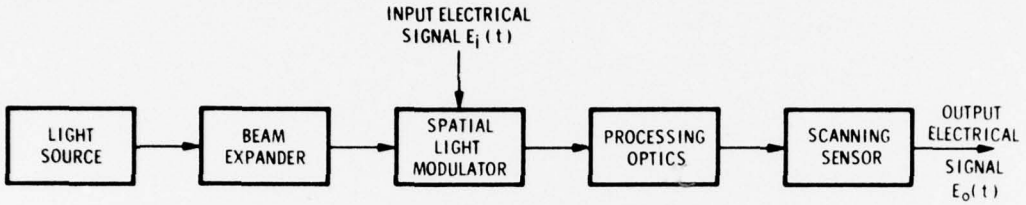

Figure 1-1. Basic Components of a Single Analog Optical Signal Processer

is used to control the properties of a spatial light modulator. This modulator is illuminated by means of a light source and beam expander with spatially coherent light, as, for example, from a laser. The output of the spatial light modulator, then, is a variable amplitude function of the x-y coordinates of the modulator. This signal enters the processing optics and may be converted back to electrical form via a scanning sensor, as for example, a Vidicon giving the output signal $E_o(t)$. The above case would cover those processing examples of linear mathematics involving, for example, spectrum analysis, filtering, etc., where a single signal input is utilized and the optical processing is a succession of one or two dimensional Fourier transformations of the initial input signal. The processing optics may store in optical form images with which the input signal is to be convolved, matched filtered or correlated. A second form of optical processer may utilize two or more electrical signal inputs and perform real-time cross correlation or other joint operation between the signals. As indicated previously, the major advantage of optical processing is the ability with the same processer to handle a multiplicity of electrical signals. Thus, several hundred input signals of the form $E_i(t)$ may be processed and demultiplexed by the scanning sensor to provide the several hundred output processed signals $E_o(t)$.

A simple example of optical processing involving the linear operation of spectrum analysis where the input signal is a function recorded on a piece of film is illustrated in Figure 1-2. The output from a laser is beam expanded and collimated into a plane wave and used to illiminate the function recorded on the film which in this case is a square wave along the x coordinate. The far field pattern from the film modulator would be approximately the Fourier transform of the amplitude function represented by the film. By placing a transform lens after the film, the Fourier transform is focused down and appears at the focal plane of the lens. For the example illustrated, the image would include a spot for the DC term representing the unmodulated light and the plus and minus fundamentals of the square wave as well as all of the odd harmonics. Since only the intensity and not the amplitude can be sensed in the image plane, it is the square of the Fourier transform that may be observed either by eye or film or as the electrical waveform at the output of a scanning sensor. However,

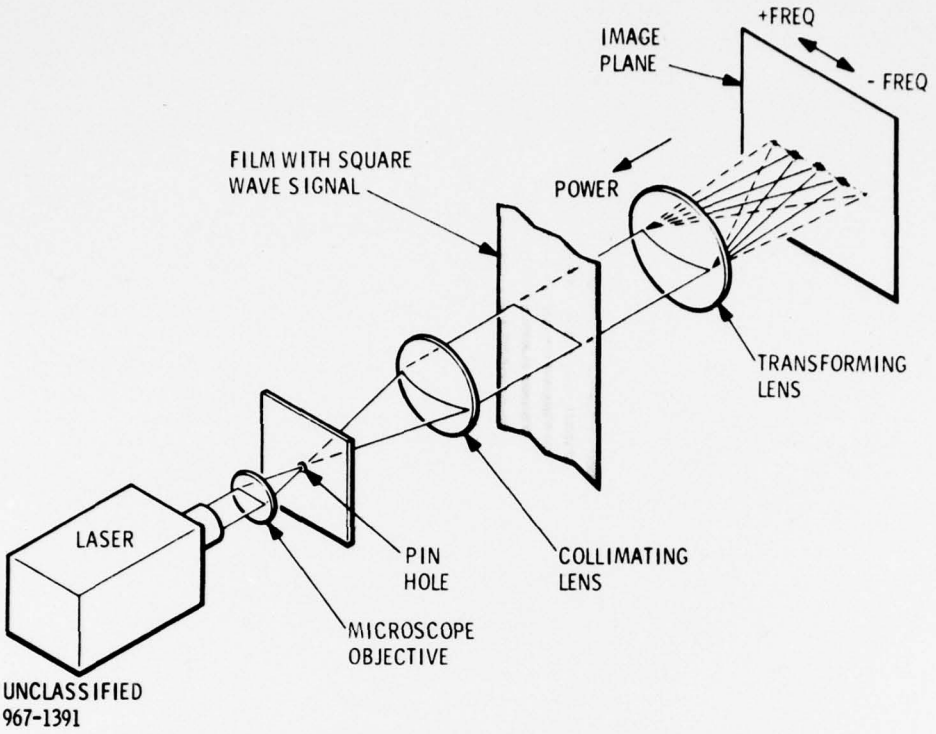

Figure 1-2. Example of Optical Processing Involving Spectral Analysis with Film as the Spatial Light Modulator

the square of the Fourier transform, $\Phi [f(x)] = \Phi(\omega)$, is $\Phi\Phi^*$ and represents a function that in its final form approximates a power spectral density which is generally of interest for spectral analysis rather than the complex Fourier transform itself. For those cases where the complex Fourier transform is desired, techniques of converting the Fourier transform to a real function may be used, as for example a reference beam (reference 3).

The magneto-optic spatial modulators replace the film in the above example and allow electrical signals to directly create the variable reflectance, thus allowing real-time processing of the input electrical information.

Specific examples of linear operations, such as spectrum analysis, which involve the Fourier transform of the input signals will be illustrated in areas as diverse as ASW signal processing, speech analysis, radar clutter processing, side-looking coherent radar mapping, and the synchronization of wideband communication waveforms.

The magneto-optic spatial light modulators developed to accomplish these processing functions are of two generic types and are covered in more detail in Appendices A and B of this report. Other modulators involving the thermo-magnetic properties of thin film are also being developed. In the first type of modulator the electrical signal is first recorded on magnetic tape which forms the storage media and is then transferred by means of the flux leakage to a thin film structure to modulate the incident light beam by means of the Kerr magneto-optic effect. This type of modulator has the advantage of extremely high packing densities (comparable with film) along with linearity and a large dynamic range (in excess of 60 db). The second type of modulator operates directly from digital information or upon analog information that has

been hardlimited and converts such signals into patterns in the thin film by means of a magnetic domain wall shifting technique. As in the first case, the optical processing utilizes changes in reflectance or rotation due to the Kerr magneto-optic effect. This approach has the advantage of eliminating mechanically moving parts required for tape transportation and achieves moderate packing densities and shifting rates in very small optical apertures. Specific applications involving these two generic types of modulators can now be discussed in more detail.

SECTION 2

MAGNETO-OPTIC SIGNAL PROCESSING APPLICATIONS

As an introduction to a variety of specific processing configurations, consider spectrum analysis where only a single transforming lens is required and where it is an extension of the example illustrated in the previous section which was based on the use of film rather than a magneto-optic spatial light modulator. This type of processer is one of the first of a series of magneto-optic signal processers under development at Magnavox Research Laboratories (reference 5). A basic magneto-optic spectrum analyzer configuration is illustrated in Figure 2-1 and consists of the following basic components:

- a spatially coherent light source
- beam expander
- a magneto-optic spatial light modulator with associated tape drive and recorder
- a diffraction limited transforming lens
- an image scanner or other readout device
- the output display

This type of processer ultilizes the type of tape transfer spatial light modulator discussed in Appendix A.

The operation of the analyzer centers on the Fourier transform properties of the light modulator and associated transforming lens such that either a one or two dimension Fourier transform is obtained in the focal plane of the lens depending upon whether the lens is pherical or cylindrical. Thus in the two dimensional case the spatial amplitude variation in the output plane is given by the following finite Fourier transform.

$$\Phi\left[f(x, y)\right] = \frac{1}{D_x D_y} \int_{\frac{-D_x}{2}}^{\frac{D_x}{2}} \int_{\frac{-D_y}{2}}^{\frac{D_y}{2}} f(x, y) \exp i\left[\omega_x x + \omega_y y\right] dx\, dy$$

where

$$\omega_x = \frac{2\pi}{\lambda F} U(u_x)$$

$$\omega_y = \frac{2\pi}{\lambda F} u_y$$

f(x, y) is the complex transmissivity of the spatial light modulator

$U(u_x)$ is nonlinear displacement in the y direction of transform plane as a fraction of spatial frequency in the signal plane due to the tilt of the plane of the spatial light

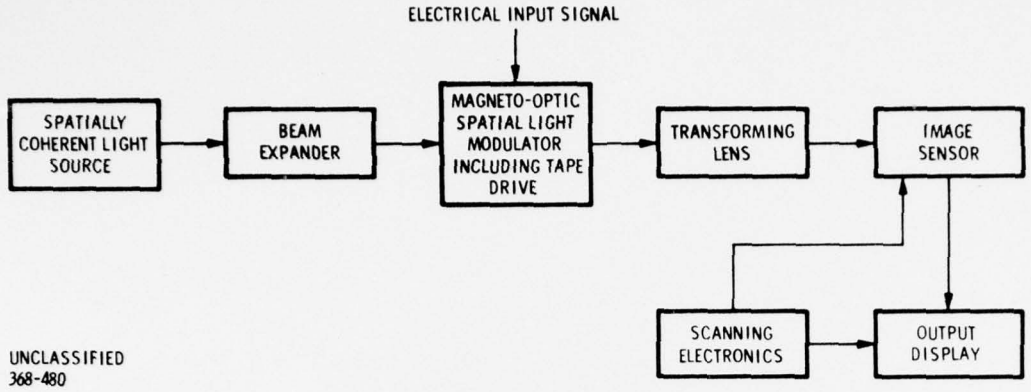

Figure 2-1. Basic Components of a Magneto-Optic System Analyzer

modulator and $\pm \frac{D_x}{2}$, $+ \frac{D_y}{2}$ are the coordinates of the aperture of the spatial light modulator. Similarly in the single dimensional case (cylindrical optics)

$$\Phi\left[f(x, y)\right] = \frac{1}{D_x} \int_{\frac{-D_x}{2}}^{\frac{D_x}{2}} f(x, y_n) \exp\left[i\omega_x x\right] dx$$

where

y_n represents the location of the n^{th} channel

The processing gain per channel of the analyzer is given by

$$PG = \frac{\Delta F}{\Delta f} = \Delta FT(D_x)$$

where

F is the rectangular equivalent input bandwidth in Hertz

f is the resolution bandwidth of the analyzer corresponding to the aperture D_x

T is the equivalent time aperture of the system (e.g., for a tape velocity, Vips, $T = D_x/V$

As a demonstration of the concepts involved, a spectrum analyzer using a standard tape recorder as a magnetic pattern generator in the magneto-optic spatial light modulator has been assembled as illustrated in the schematics and photographs of Figure 2-2 and 2-3. This configuration uses an inexpensive Vidicon camera and monitor for viewing the spatial spectral density in the analyzer output or transform plane. Various signals were recorded to illustrate the parameters of this specific processer and may be displayed either as a full Fourier transform or in a relative power versus frequency format corresponding to an amplitude section of a standard spectrogram as illustrated in Figure 2-4.

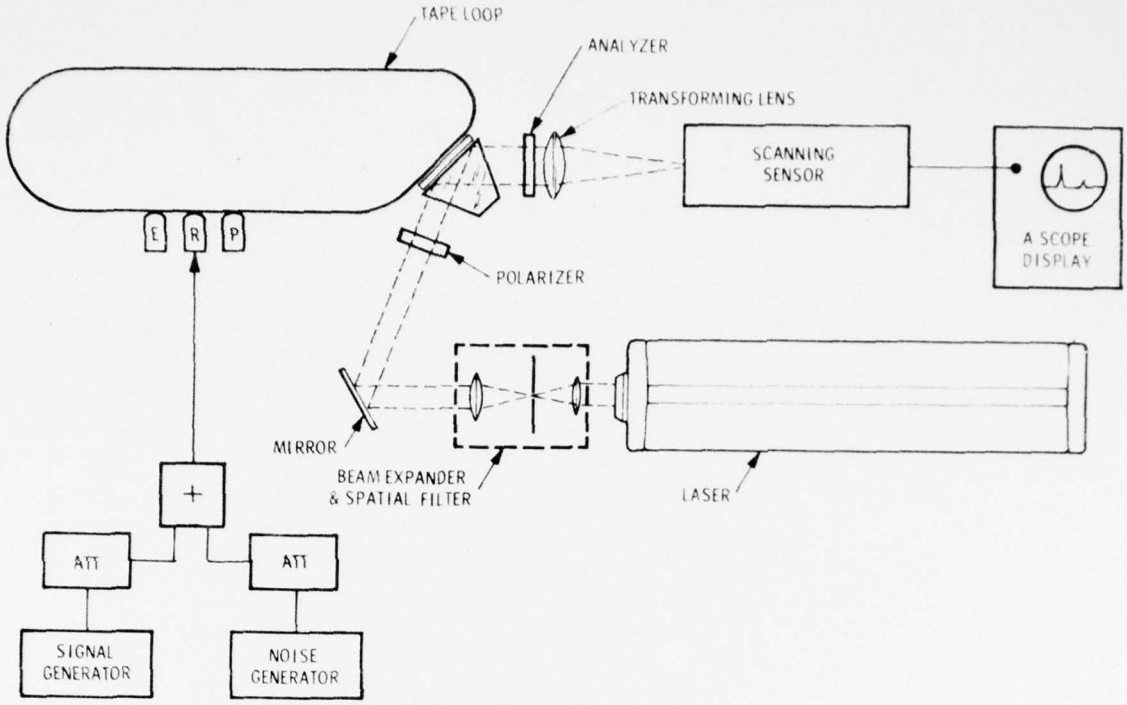

UNCLASSIFIED
268-376

Figure 2-2. Schematic of Demonstration Spectrum Analyzer

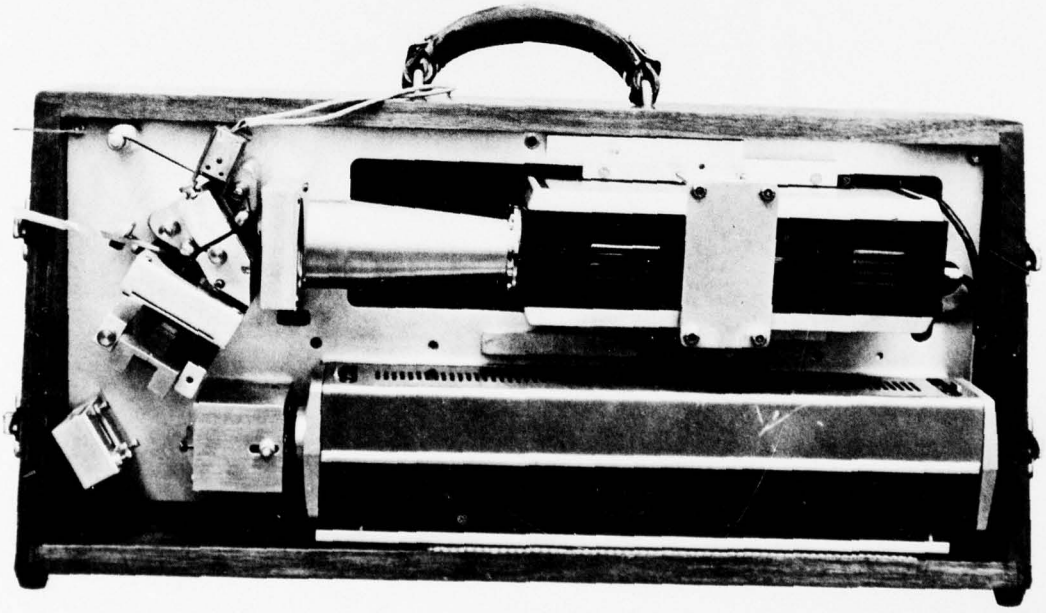

UNCLASSIFIED
268-377

Figure 2-3. Demonstration Spectrum Analyzer

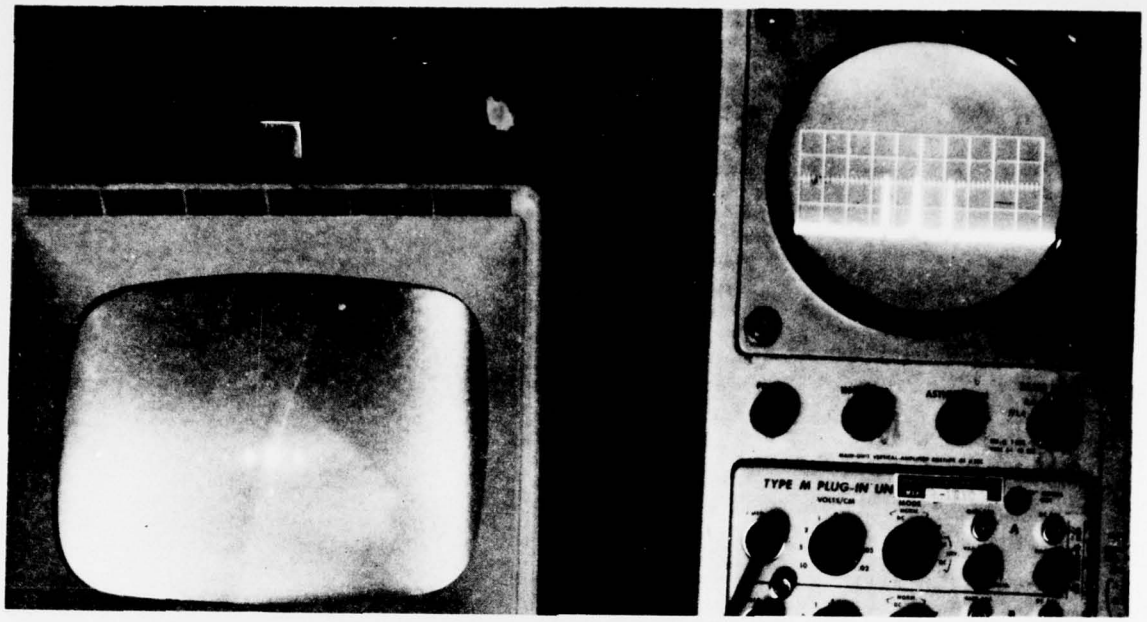

UNCLASSIFIED
967-1595

Figure 2-4. Two Different Displays of the Fourier Transform Squared ($\Phi\Phi^*$) From Magneto-Optic Spectrum Analyzer

A convenient test signal is the ideal pulse train and its associated power spectrum as illustrated in Figure 2-5. This test signal is useful in determining the resolution of the analyzer. A similar signal and a 4-KHz test tone were used to illustrate the operation of the demonstration analyzer. The results of this test are illustrated in Figure 2-6 along with the result from a spectrogram obtained from a commercial spectrum analyzer (Kay Model 6061A Spectrum Analyzer). The output display is obtained directly from the scanning sensor and fed to a laboratory oscilloscope. The vertical axis in this display represents relative power or power spectral density, while the horizontal axis represents the frequency domain.

Signals were also recorded with noise to illustrate the processing gain of the analyzer. The results for this case are illustrated in Figure 2-7 where the noise is from a 6 KHz rectangular equivalent noise bandwidth and the processing gain of the analyzer is set for approximately 20 DB. The signal to noise ratios quoted are those appearing at the input of the analyzer in the 6-KHz bandwidth.

2.1 ASW PROCESSING

While the above examples have involved a relative power versus frequency format, the nature of the readout allows a flexibility in the output format. For example, a time versus frequency format is easily arrange. Figure 2-8 illustrates such a format

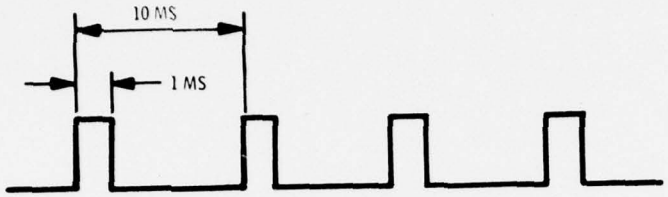

INPUT PULSE TRAIN TEST SIGNAL TO SPECTRUM ANALYSER

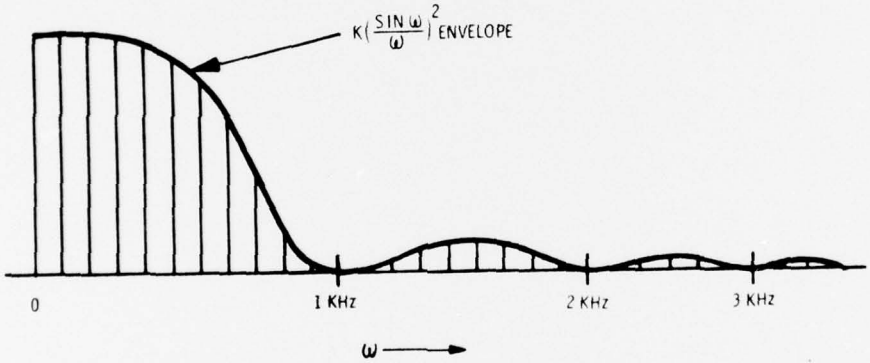

IDEAL POWER SPECTRUM OF INPUT PULSE TRAIN.

UNCLASSIFIED
1167-2457

Figure 2-5. Ideal Pulse Train Test Signal and its Power Spectral Density

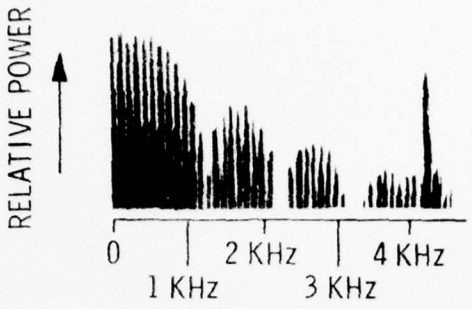

CONVENTIONAL NARROWBAND (45 Hz) SPECTRAGRAM OF PULSE TRAIN (0 DB IN VU) AND 4 KHz TEST TONE (-5 DB IN VU) (FL-1; AGC-10; ML-9)

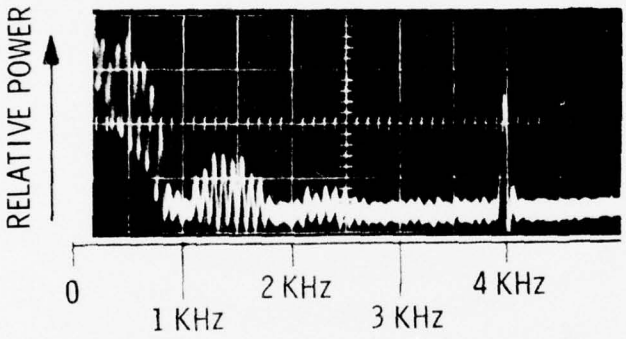

MAGNETO-OPTIC NARROWBAND SPECTROGRAM OF PULSE TRAIN (0 DB IN VU) AND 4 KHz TEST TONE (-5 DB IN VU).

UNCLASSIFIED
1167-2421

Figure 2-6. Spectra Of Pulse Train Test Signal on Commercial and Magneto-Optic Spectrum Analyzers

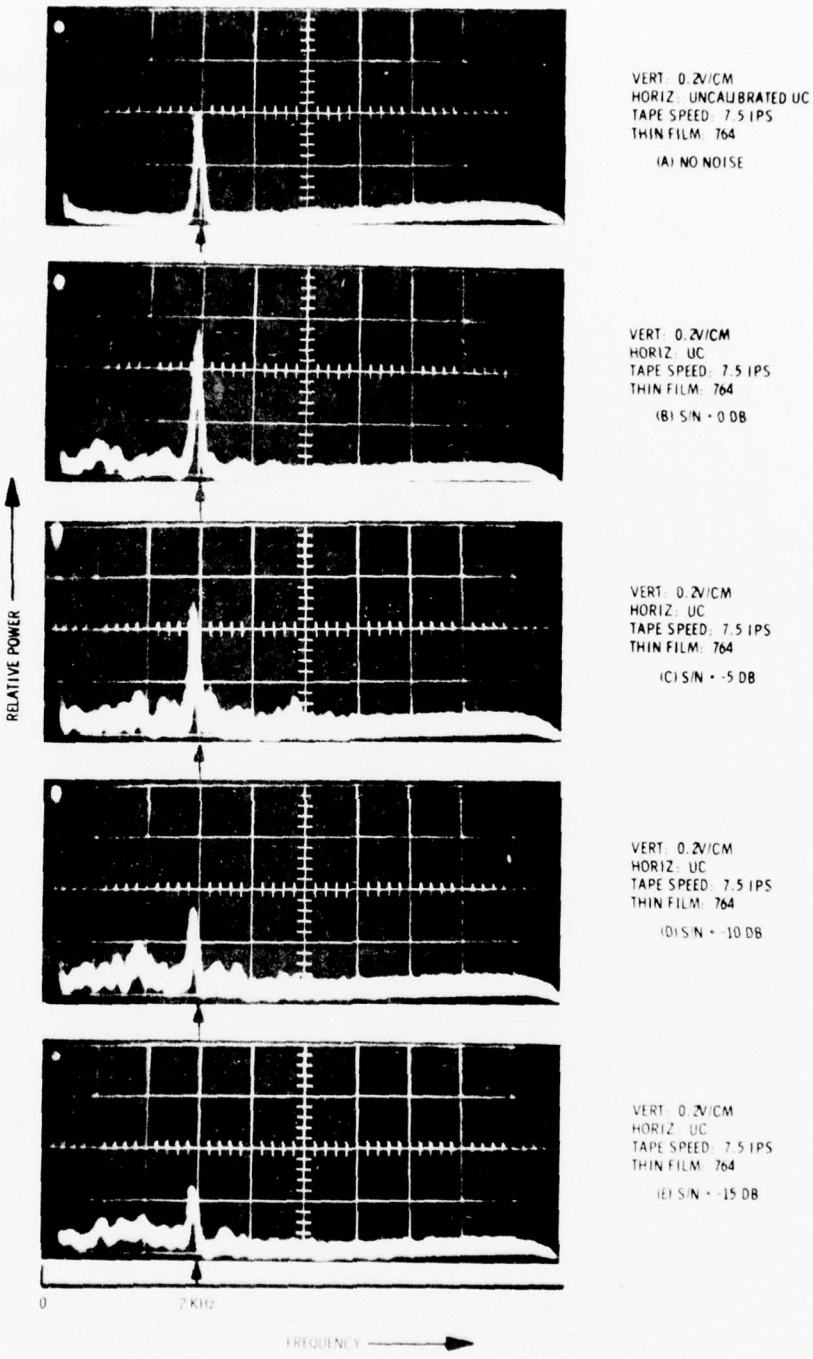

Figure 2-7. Spectrogram Illustrating the Processing Gain of A Demonstration Spectrum Analyzer

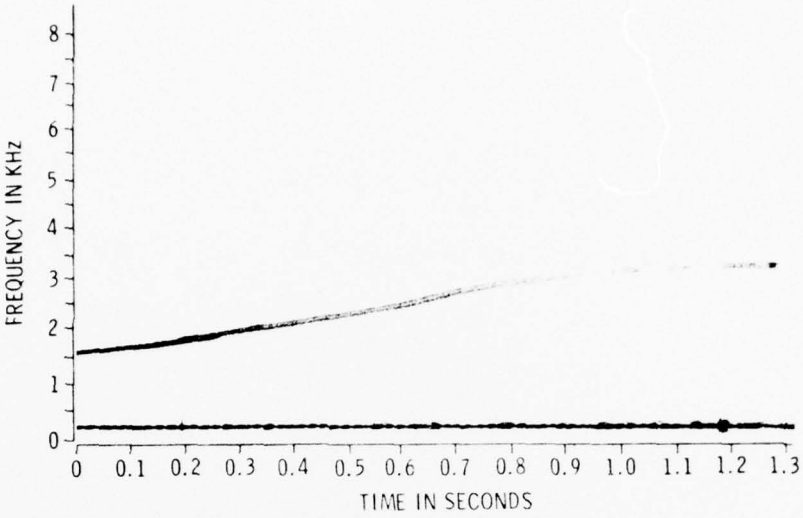

CONVENTIONAL NARROWBAND SPECTROGRAM OF FREQUENCY RAMP.

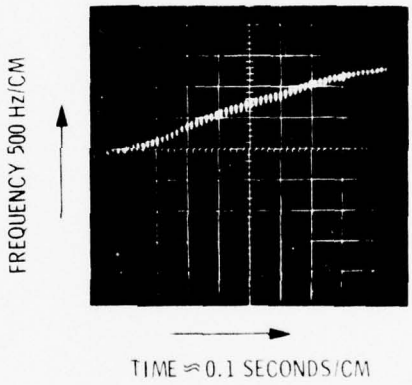

MAGNETO-OPTIC NARROWBAND SPECTROGRAM OF FREQUENCY RAMP.

UNCLASSIFIED
1167-2425

Figure 2-8. Conventional and Magneto-Optic Narrowband Spectrogram of a Frequency Ramp

for a signal whose frequency varies with time on both a conventional spectrum analyzer and a magneto-optic spectrum analyzer. In this case the magneto-optic spectrum analyzer gives a sampled output at a 60-Hz rate since a conventional Vidicon scanning field was utilized in the readout. Such a format is often used in ASW systems and corresponds to a LOFARGRAM.

2.1.1 BEARING COMPUTATION

Other ASW and also RF processing functions such as bearing determination depend on spectral analysis for processing gain. The signal flow for such a processor is illustrated in Figure 2-9, and an estimation of the required physical configuration is illustrated in Figure 2-10.

2.1.2 BEAM FORMING

Another linear operation frequently encountered in ASW processing is the weighted summation found in beam forming activities such as those represented by Digital Multiple Beam Steering DIMUS (references 6 and 7). Such beam forming may be accomplished magneto-optically by either coherent or noncoherent techniques. In the coherent case, either a scanned or parallel replica of the acoustic wavefront is sampled and stored on tape. A coherent reconstruction of either the object or its transform is possible and represents essentially a holographic approach. A somewhat simpler approach and one that does not require the resolution capabilities of tape nor does it require any moving parts is a noncoherent processor based on the magnetic domain wall shift register type of modulator discussed in Appendix B. The separate hydrophone outputs may be fed to individual magneto-optic domain wall shift register channels. Thus, for a linear array where the angle of the wavefront is α and the velocity of propagation V_1, the velocity of propagation in the register V_2, may be adjusted so that a summation of the signal appearing at an angle α_2 across the separate channels represents the original wavefront as illustrated schematically in Figure 2-11. If the light is collected separately from different masks a multibeam processor is possible. Effectively such an approach is identical to the standard DIMUS technique except that the weighting network and signal interconnecting is accomplished optically instead of by wire and discrete component weighting networks. A typical electrical readout of a single channel for such a shift register is illustrated in Figure 2-13. For large configurations, the hardware savings realized by the optical versus electronic approach can be considerable and offer a solution where the large-scale integration (LSI) wiring interconnection problem is of such a magnitude as to preclude a practical solution. For simple linear arrays, the extension to coherent optics allows some simplification, for example, the angle preserving properties of the Fourier transform allows partitioning of the separate waveform outputs in the transform plane. Such a configuration is illustrated in Figure 2-12.

2.2 SPEECH PROCESSING

The general spectrum analyzer configuration introduced at the beginning of this section has a multiplicity of uses: for example, consider the spectrograms of Figure 2-14 resulting from steady state speech samples. These particular speech samples illustrate the first three formants of the vowel "æ" from as "a" in "at."

In order to interpret the power density and frequency axes, calibration curves must be applied to the readout device. In the particular spectrogram of Figure 2-14, the relative power axis was limited to approximately 20 db due to characteristics of the Vidicon used as the scanning sensor. Narrowband spectrograms of other typical speech samples are illustrated in Figure 2-15.

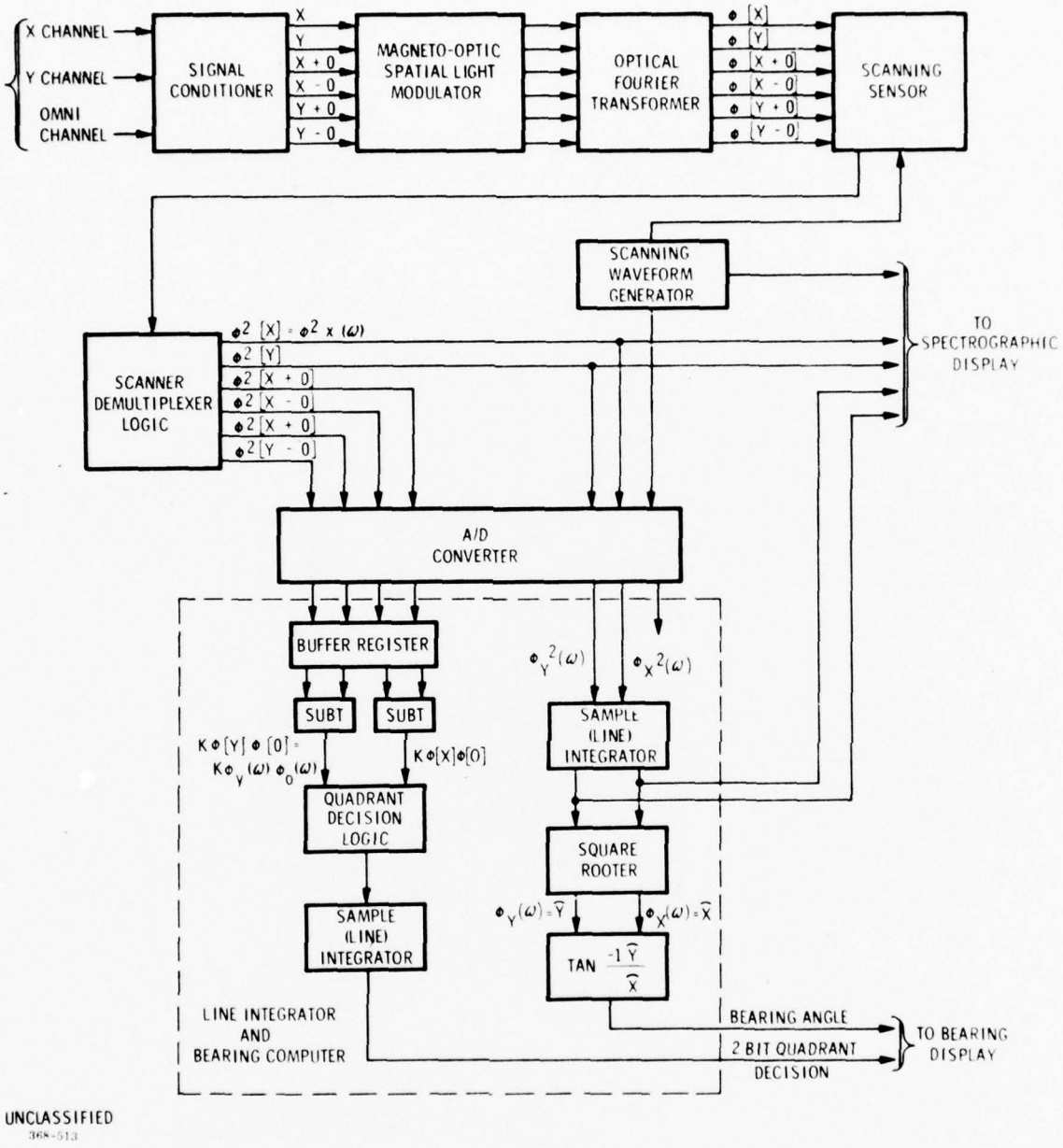

Figure 2-9. Signal Flow for a Magneto-Optic Bearing Computer Utilizing Spectrum Analysis

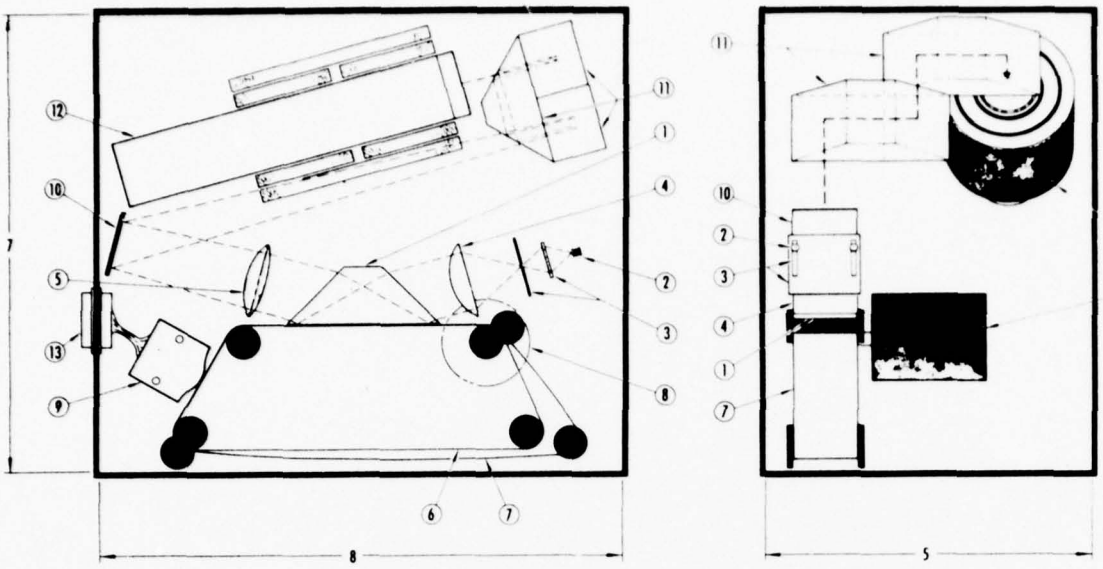

1 PRISM AND MAGNETO-OPTIC THIN FILM
2 GaAs LASER ARRAY
3 CYLINDRICAL LENS ARRAY & PINHOLES
4 CYLINDRICAL COLLIMATING LENS
5 CYLINDRICAL TRANSFORMING LENS
6 AREA TAPE DRIVE BELT & TENSION CONTROL
7 TENSION-FREE 2 INCH TAPE LOOP
8 AREA DRIVE CAPSTAN
9 MULTICHANNEL TAPS RECORD HEAD
10 SURFACE MIRRORS
11 PRISMS
12 MINIATURE VIDICON DRIVE & FOCUS COILS
13 CONNECTOR TO RECORD HEAD
14 MOLDED LOG CORRECTOR PLATE

UNCLASSIFIED
767-1140D

Figure 2-10. Magneto-Optic Bearing Computer Physical Configuration

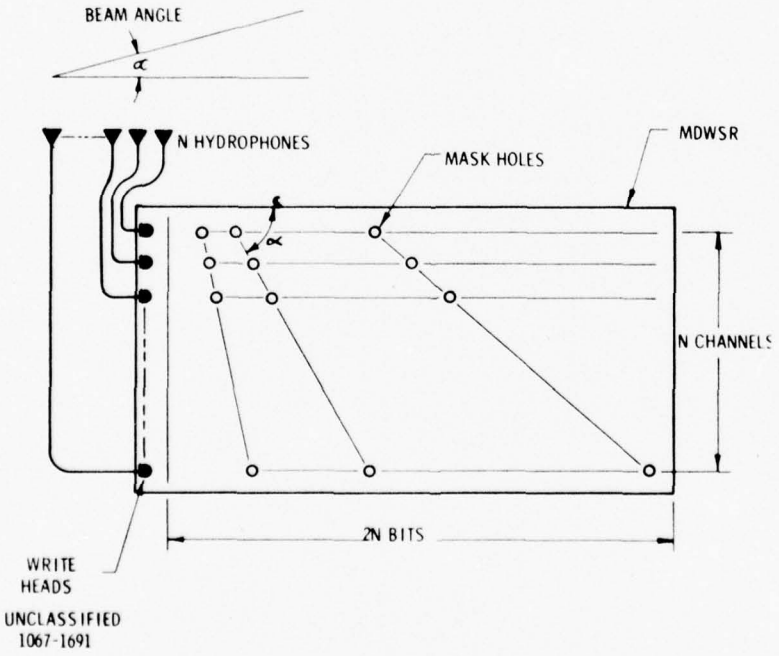

UNCLASSIFIED
1067-1691

Figure 2-11. Concept of ASW Beam Forming with the Magneto-Optic Readout of a Linear Sensor Array in a Magnetic Domain Wall Shift Register

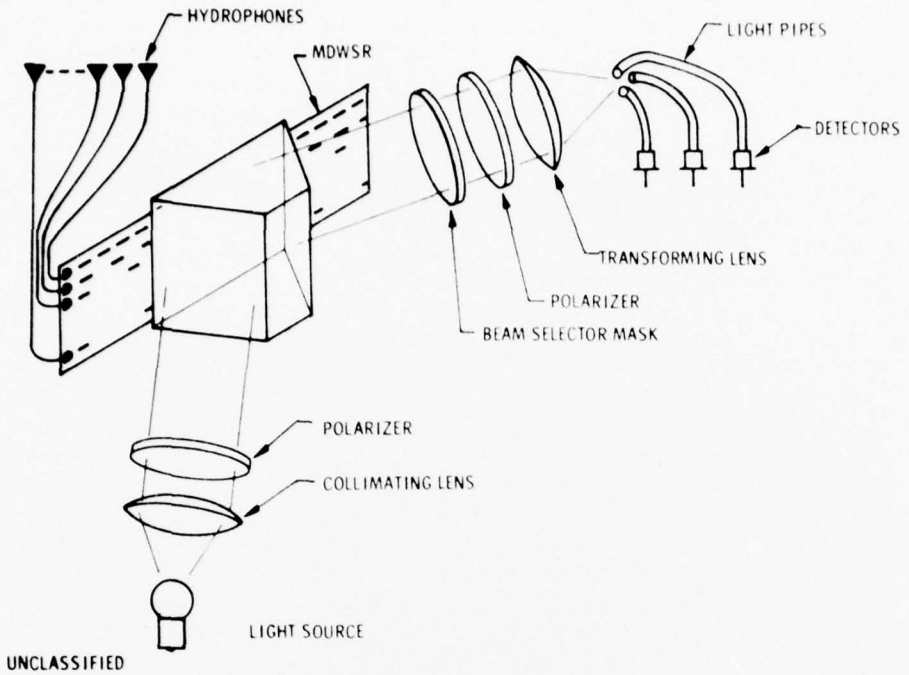

Figure 2-12. Coherent Beam Forming From a Linear Array Utilizing Magnetic Domain Wall Shift Register

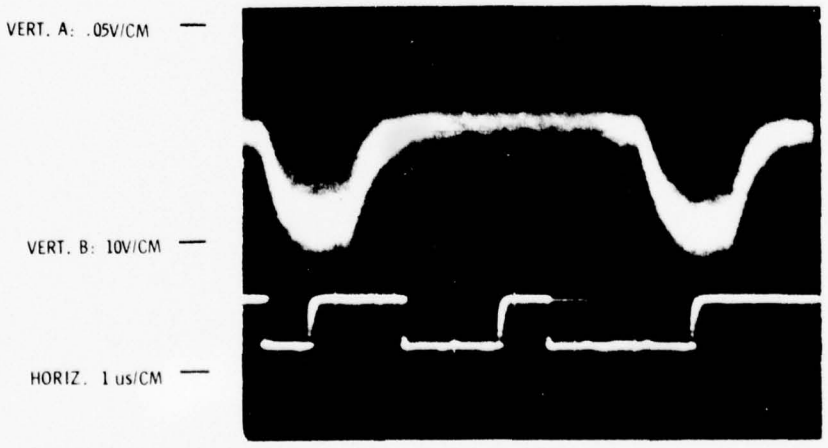

Figure 2-13. Electrical Readout from a Magnetic Domain Wall Shift Register Suitable as a Non-Coherent Beam Forming Component

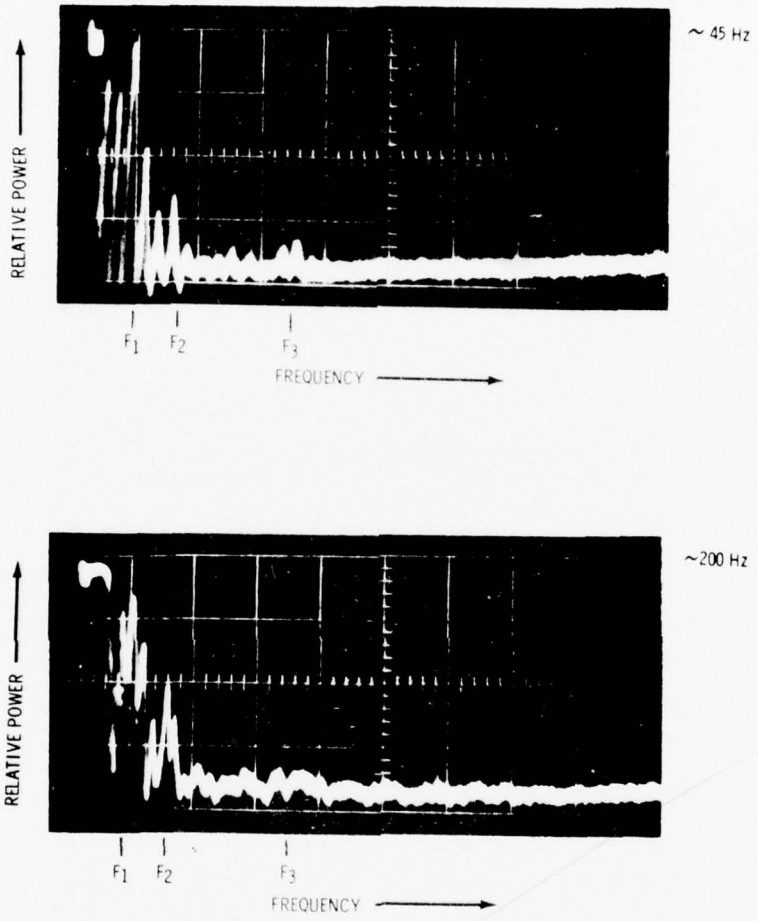

Figure 2-14. Amplitude Sections of Phoneme "ō" from "Whale" with Narrow (~45 Hz) and Wideband (~200 Hz) Analysis Bandwidths

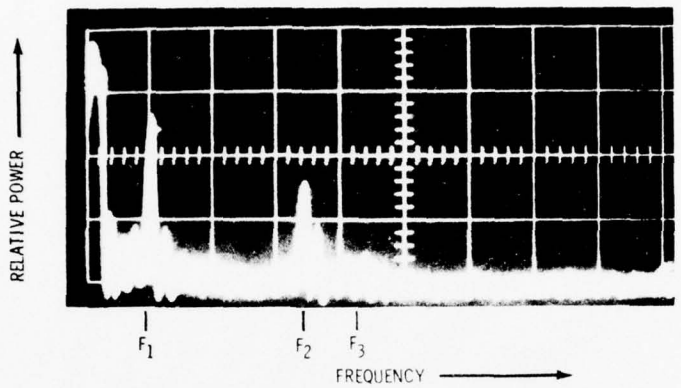

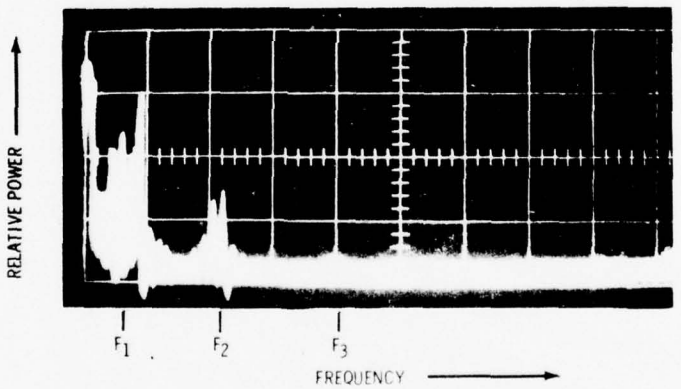

UNCLASSIFIED
368-529

Figure 2-15. Typical Amplitude Sections of Speech Samples Showing Formats and Pitch Harmonics Analysis Bandwidth Approximately 45 Hz

While laboratory versions of spectrum analyzers similar in volume to the demonstration analyzer that is illustrated in Figure 2-3 may be constructed, the use of solid state components for the light source and scanning sensor can reduce the total configuration to a few cubic inches. An example of the reduction possible is illustrated for a cepstrum analyzer in Figure 2-16. The cepstrum is defined as a Vidicon proportional to the Fourier transform of the log spectrum (reference 8). This analyzer represents an analog version of a compact and inexpensive Fast Fourier transform device with the capability of handling up to eight channels simultaneously. A two channel device for the extraction of pitch information in speech is illustrated by the functional diagram of Figure 2-17. A third channel could be used to extract the formant information for a channel type of vocoder.

2.3 RADAR CLUTTER PROCESSING

Another intriguing example of spectrum analysis use is for the clutter processing of radar information. The operation of the clutter processer again depends on only a single cylindrical transform lens. The input signal to the spatial light modulator is arranged in a range-time format as indicated in Figure 2-18. A transverse tape head drum records across the tape in correspondence with the range return from the radar. Thus, constant range represents a longitudinal track on the tape. Taking the Fourier transform in the direction of the tape motion or azimuth produces a two-dimensional display in which the intensity (Z) axis represents the square of the Fourier transform while the X and Y axes represent variables of velocity (corresponding to frequency) and range respectively. The output spectrum from this format may be observed visually in the focal planes of the transform lens or converted to an appropriate video signal by a Vidicon or other scanning sensor. With a cylindrical transforming lens as many channels may be handled in parallel as can be placed on the tape and within the optical aperture. In the case of the clutter processer, the parallel channels represent the various range bins. With a transverse recording head, several hundred channels to the inch may be obtained.

As a demonstration of the concepts involved, a clutter processer utilizing the transverse record head illustrated in Figure 2-19 and standard video tape is being assembled according to the block diagram and schematic of Figure 2-20 and 2-21 (reference 9). Preliminary results from a video simulator give the spatial functions for the signal and transform planes illustrated in Figure 2-22 and 2-23 respectively for a target of essentially constant range within a gross range bin but with a doppler shift that is proportional to the instantaneous target velocity. In practice, the processer must exhibit processing against a clutter return similar to that indicated in Figure 2-24.

2.4 COHERENT SIDELOOKING RADAR PROCESSER

A processer configuration closely associated with the clutter processer, in as much as it utilizes the same format of data into the spatial light modulator, is a coherent sidelooking radar processer or mapper. The description of such a mapper utilizing film has been converted by Cutrona (reference 10 and 11). Effectively the radar return can form a line by line hologram of the ground return. The output image may be formed reconstructing the hologram in the azimuth direction and using the inherently high resolution of the range return either by short pulses or more efficient wideband phase shift modulation, to portray the range dimension. A result similar to that illustrated in Figure 2-25 (from reference 11) may be obtained by the configuration illustrated in Figure 2-26. The requirements for the optics necessary to image a high resolution ground return are similar to those described by references 10 and 11

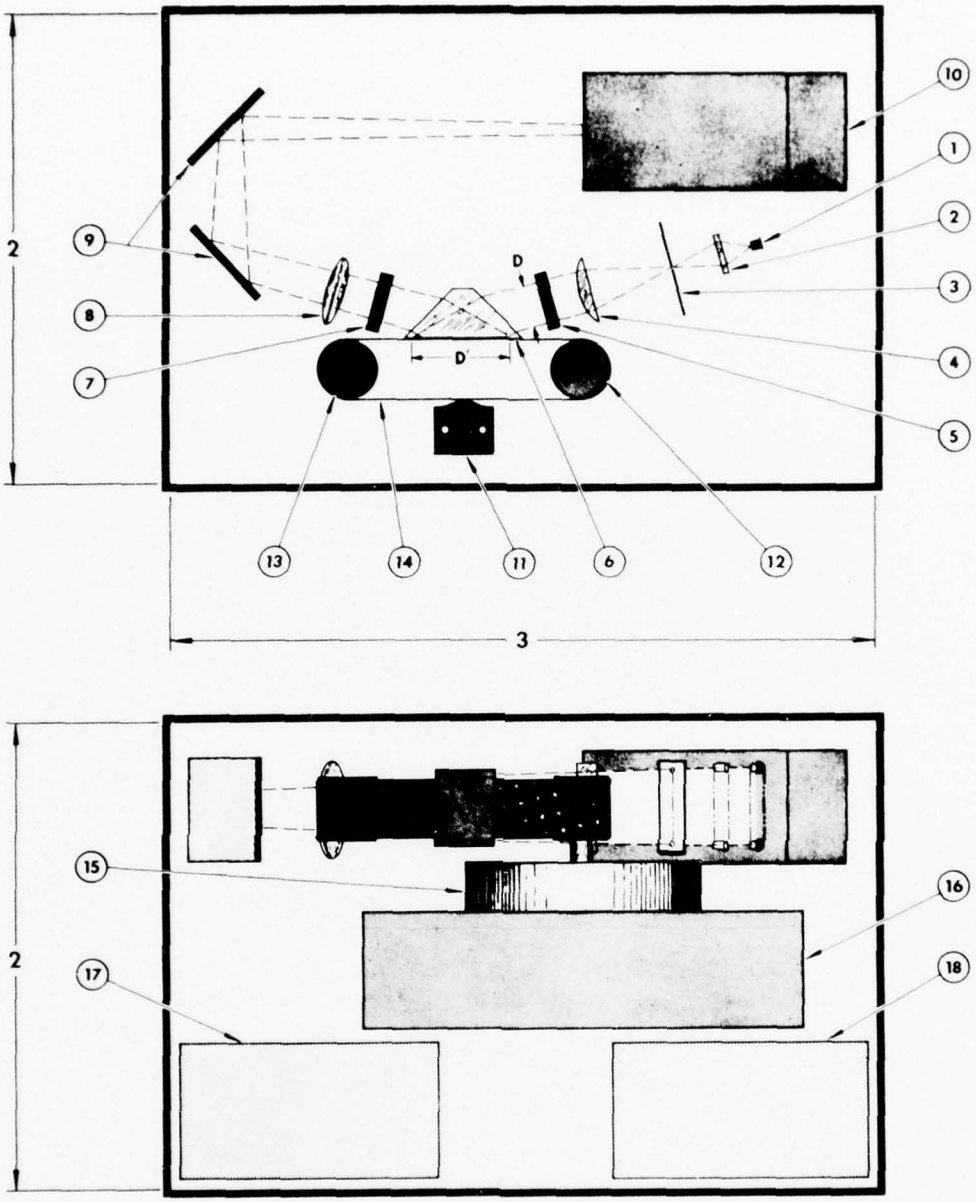

1 SOLID STATE GaAs LASER IN TO-46 CAN
2 CYLINDRICAL LENS
3 PIN HOLE
4 CYLINDRICAL COLLIMATING LENS
5 POLARIZER
6 PRISM AND THIN FILM
7 ANALYZER
8 CYLINDRICAL TRANSFORMING LENS
9 SURFACE MIRROR
10 SOLID STATE SCANNING SENSOR ARRAY (125 ELEMENT)
11 2-CHANNEL ERASE/RECORD HEAD
12 CROWN CAPSTAN
13 CROWN TENSION IDLER
14 TEFLON COATED SEAMLESS TAPE LOOP
15 FLYWHEEL
16 PANCAKE PRINTED CIRCUIT MOTOR
17 RECORD ELECTRONICS
18 ERROR SIGNAL AND ACQUISITION ELECTRONICS

UNCLASSIFIED
268-343

Figure 2-16. Conceptual Drawing of an Analog Fast Form Transformer Used as a Cepstrum Analyzer

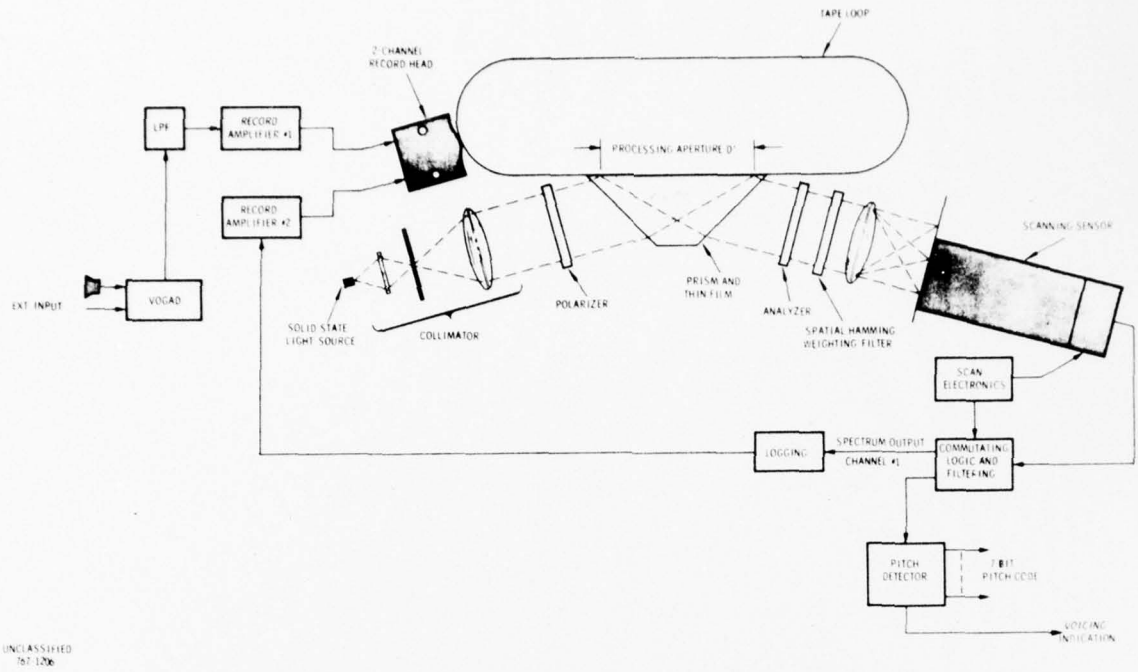

Figure 2-17. Functional Diagram of Magneto-Optic Cepstrum Pitch Extraction

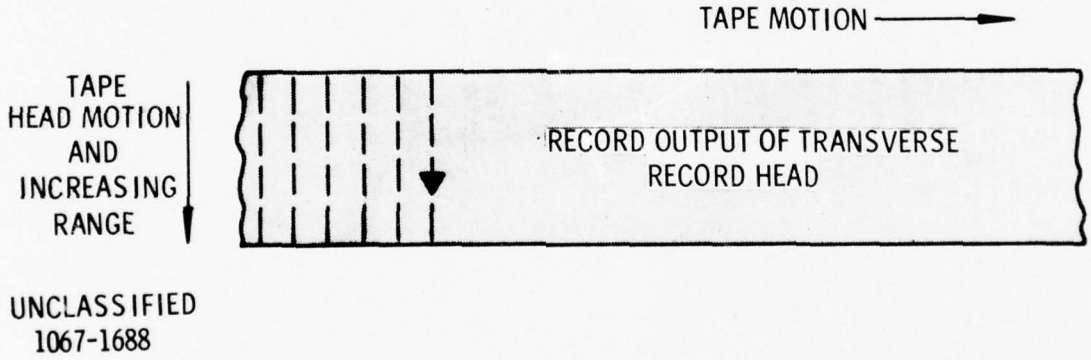

Figure 2-18. Format of Video Data on Spatial Light Modulator Tape Loop

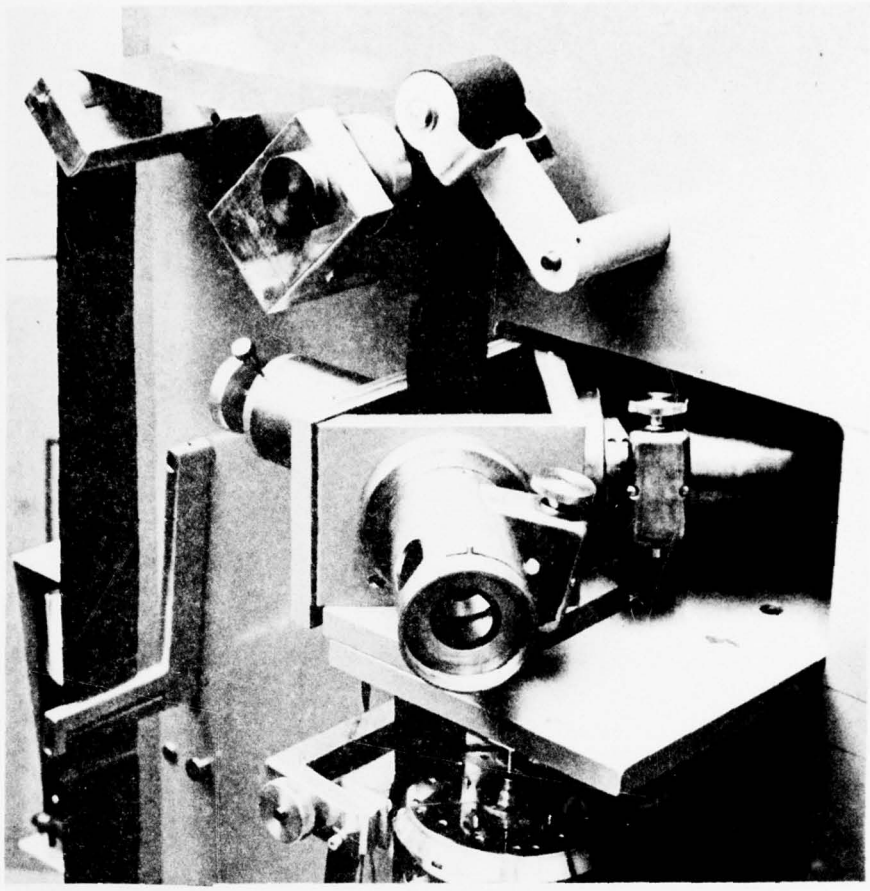

UNCLASSIFIED
767-1136

Figure 2-19. A High Density Transverse Record Head and Spatial Light Modulator

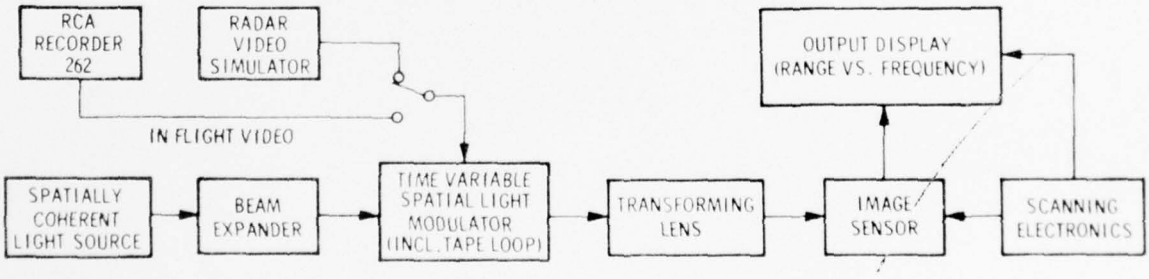

UNCLASSIFIED
168-220

Figure 2-20. Basic Components of a Magneto-Optic Clutter Processor

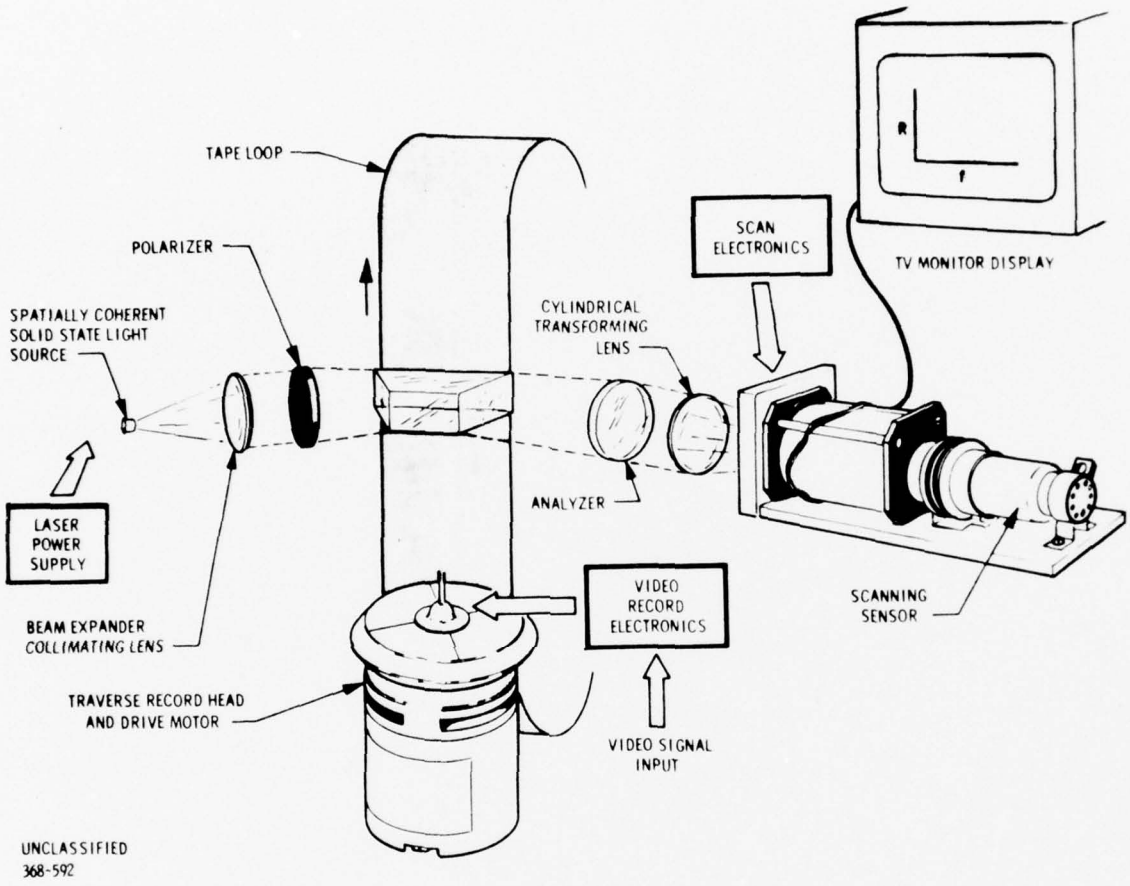

Figure 2-21. Schematic of Demonstration Radar Clutter Processer

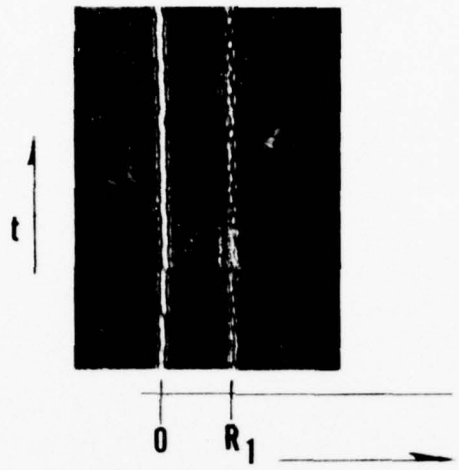

UNCLASSIFIED
668-1215

Figure 2-22. Simulated Radar Video in Plane of Spatial Light Modulation

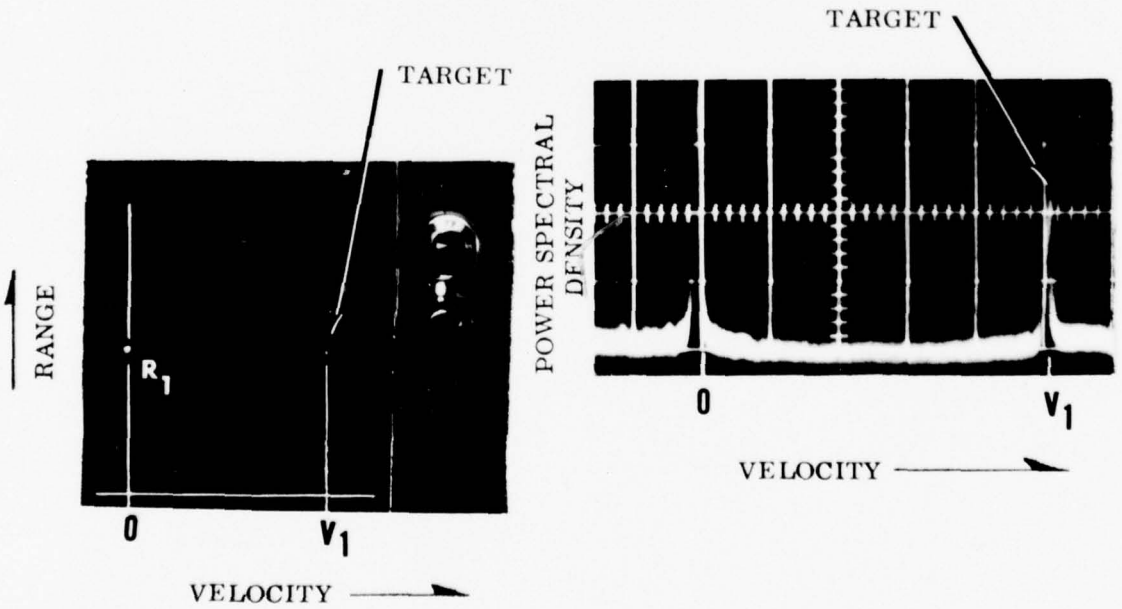

UNCLASSIFIED
668-1216

Figure 2-23. Simulated Radar Video in Transform Plane of Clutter Processer

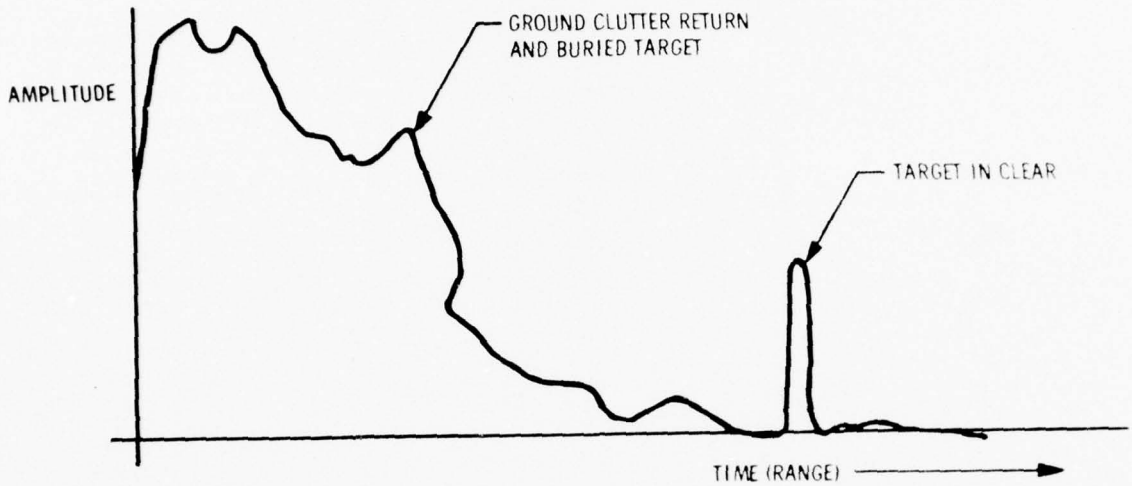

UNCLASSIFIED
368-551

Figure 2-24. Radar Ground Clutter Return with Buried and Clear Targets

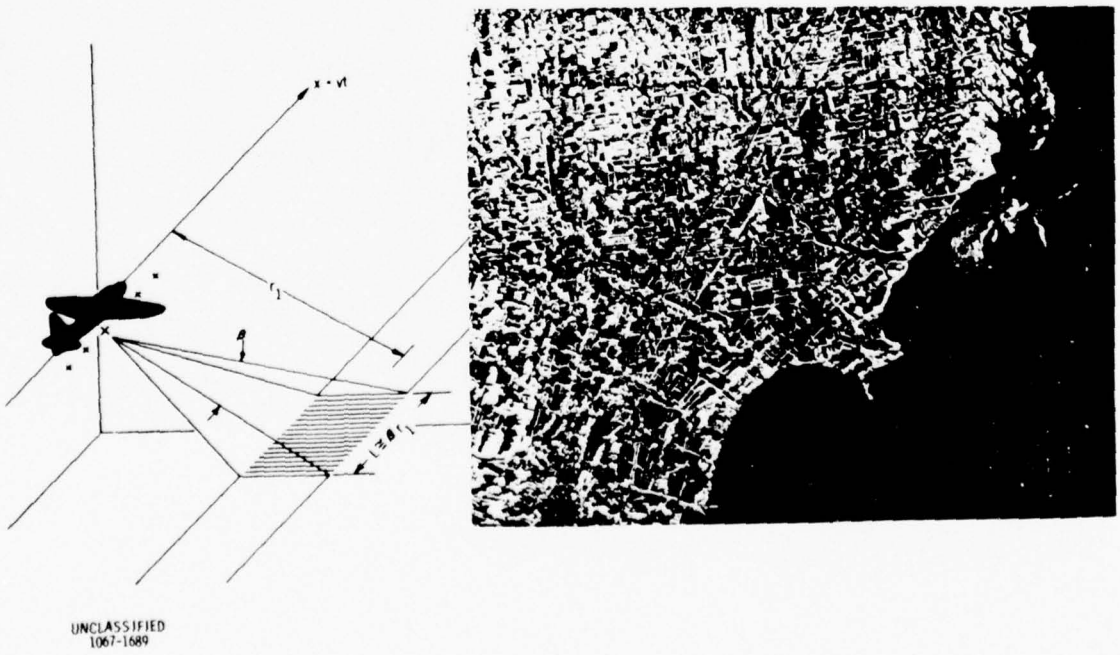

UNCLASSIFIED
1067-1689

Figure 2-25. Coherent Sidelooking Radar Mapper Output (Reference 11)

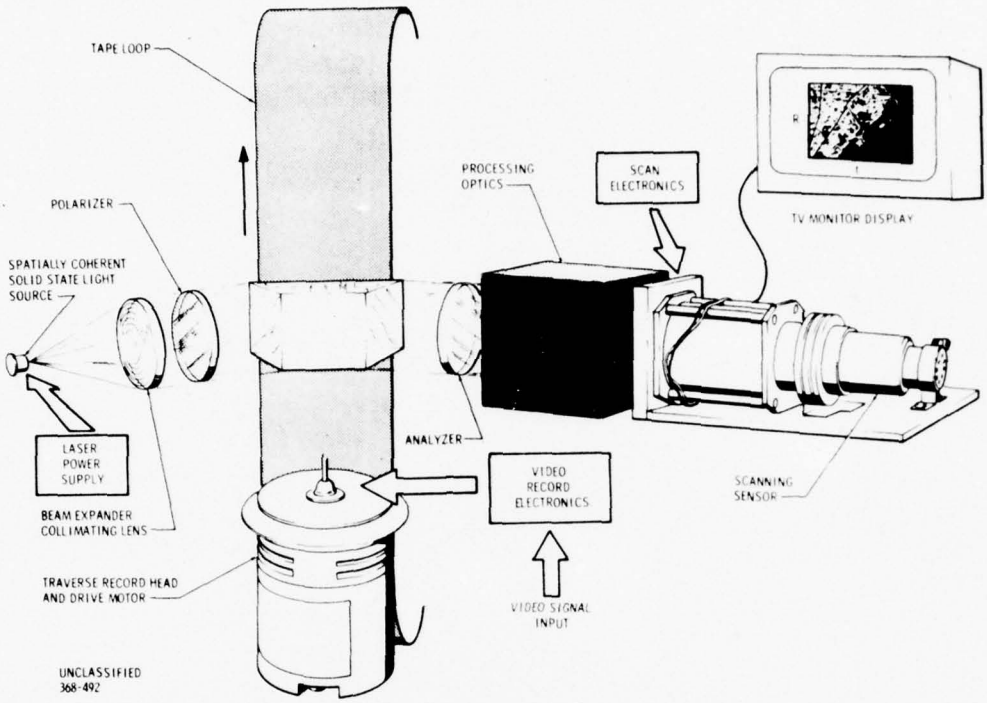

Figure 2-26. Schematic of Coherent Sidelooking Radar Mapper

but must take into account the non-linear scale factor introduced by tilting the spatial light modulator plane (reference 12). In this case the processing optics consist of a wedge corrector plate: to counteract the effect of the spatial light modulator tilt: a conical lens of variable focal length and aperture to give an erect image (at infinity) and constant resolution to the azimuth information: a cylindrical lens to place an image of the range information at infinity: and a spherical lens to image the reconstructed waveform at the scanning sensor. Such a processer allows real time readout of the ground map at a resolution consistent with the resolution available from real-time cockpit displays.

2.5 TWO-DIMENSIONAL FOURIER TRANSFORMS

Other configurations involving a two-dimensional spectral analysis are possible. For example, if the signal is recorded on tape by a transverse record head, the two-dimensional Fourier transform will indicate components that are a function both of the transverse track separation in the direction of tape motion and the recorded signal spectrum in the direction of record head motion. Such a spectrogram is illustrated in Figure 2-27 where the x axis corresponds to spatial frequencies in the direction of head motion and the y axis corresponds to spatial frequency in the direction of tape motion. A calibration curve for the x spatial frequency axis is illustrated in Figure 2-28 where the nonlinearity of the scale factor due to tilt of the spatial light modulator may be observed. Such a technique is applicable to the real-time analysis of RF signals.

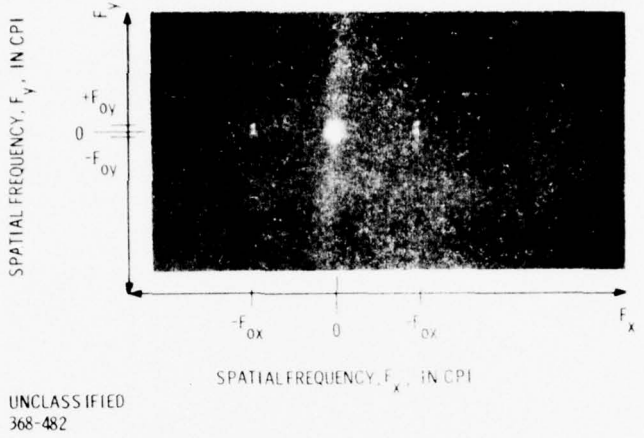

Figure 2-27. Two Dimensional Fourier Transform of Signal Recorded Transverse Record Format

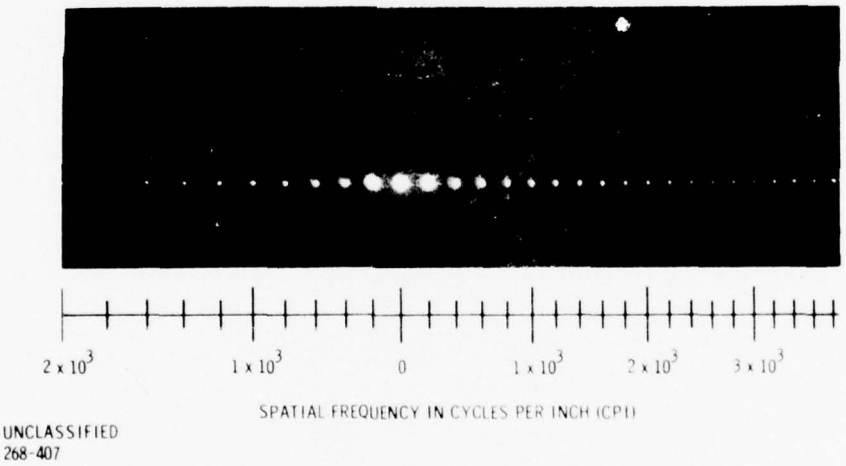

Figure 2-28. Calibration Curve Illustrating Variation of Spatial Frequency In Transform Plane for Spatial Light Modulator Tilted at an Angle of Incidence, $\alpha = 60°$

The list of particular processing applications may be quite long, for example, Figure 2-29 illustrates the two-dimensional transform of a signal representing the output of an airframe accelerometer. Since the signal in this is essential of a single dimension, the result as it appears is equivalent to a single dimensional transform.

2.6 COMMUNICATION SYSTEM PROCESSING

While tactical vocoders based on a magneto-optic cepstrum analyzer offer a potential in voice communications, the emphasis in the communication area has classically centered on correlators for such diverse functions as identification friend or foe (IFF), synchronization, and data demodulation. To this end, both non-coherent and coherent magneto-optic correlation and spectrum analyzer configurations have been under investigation at Magnavox Research Laboratories (references 13 and 14).

Correlation processers differ from the previous processing configurations considered in that two time varying signals may be entered into the processer. A basic optical correlator configuration illustrating this property is given in Figure 2-30. The received signal plus noise waveform generally enters the correlator at intermediate frequency (IF) level and is converted to a spatially variable intensity pattern by means of the signal interface electronics and the X spatial light modulator. For the moment, the spatial light modulator may be treated as if it were a piece of film created in real-time from the input signal plus noise waveform. T seconds worth of this signal is then presented to the light source. The light source after collimation passes through the spatial light modulator. Transform optics and spatial filtering follow and reconstruct the signal presenting it to the surface of a second or Y, spatial light modulator. This spatial light modulator represents T seconds of the stored reference signal which is either fixed in the case of a classical "matched filter" or is variable as in a time-varying "matched filter". The variation is a function of the selected scan method. The light passing through both the X and Y spatial light modulators effectively multiplies T seconds worth of the input and stored reference signals. The final optics following the multiplication then Fourier transforms the product and is equivalent to T seconds of integration in an electronic correlator. At an appropriate location in the output spatial domain, the correlation function of T seconds worth of the incoming signal plus noise waveform with T seconds worth of the stored reference signal is available.

Specific configurations illustrating both the classical fixed stored reference "matched filter" and the variable time-varying "matched filter" have been investigated for both non-coherent and coherent structures.

A basic configuration for a non-coherent magneto-optic matched filter is illustrated in Figure 2-31. The X spatial light modulator, consisting of a polarizer, magnetic domain wall shift register, and analyzer, converts the input light polarized in the plane of incidence (for the Kerr longitudinal magneto-optic effect) into a spatial light amplitude pattern that is a function of the analyzer angle, α. In the simplest case the Y spatial light modulator is a piece of film on which the desired reference signal is stored. In practice the reference signal can be made by stopping the desired pattern in the X spatial light modulator and photographing the results. When developed and reversed, the film may then be replaced in the correlator as the spatial reference signal. With cylindrical optics several different reference signals may be stored on the same film and the output image plane examined by a light sensing array or scanner to determine which stored reference correlates most strongly with the incoming signal. The major advantage in the use of film for the Y light modulator lies in its low insertion loss. However, processing in a non-coherent mode introduces error terms

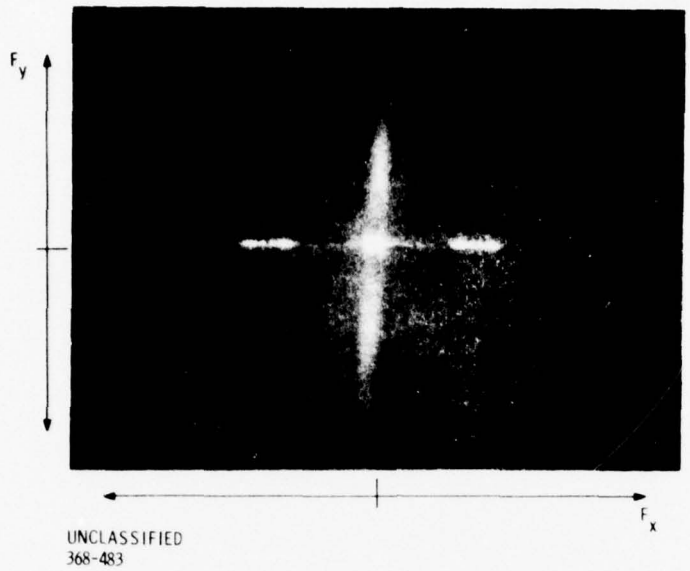

Figure 2-29. Two Dimensional Transform of a Single Dimensional Signal from an Accelerometer Output

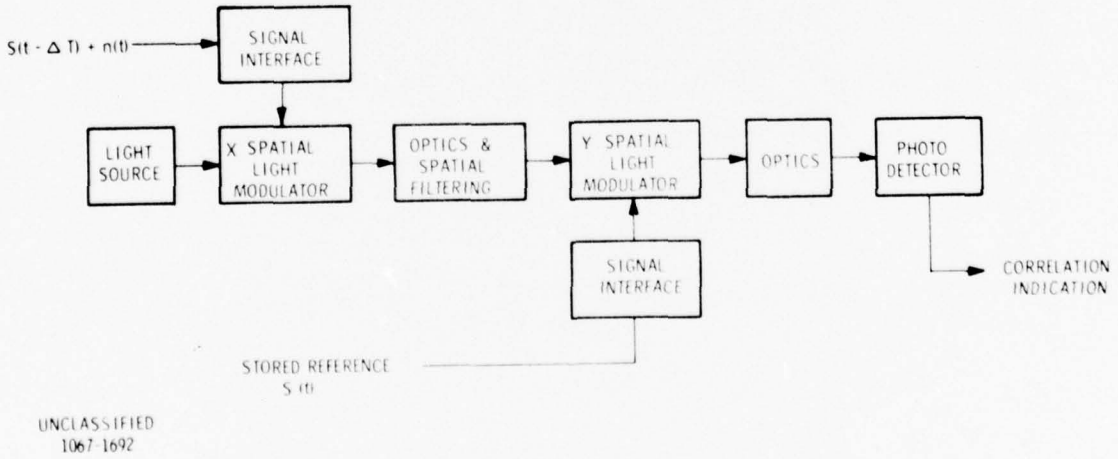

Figure 2-30. Basic Optical Correlator Configuration

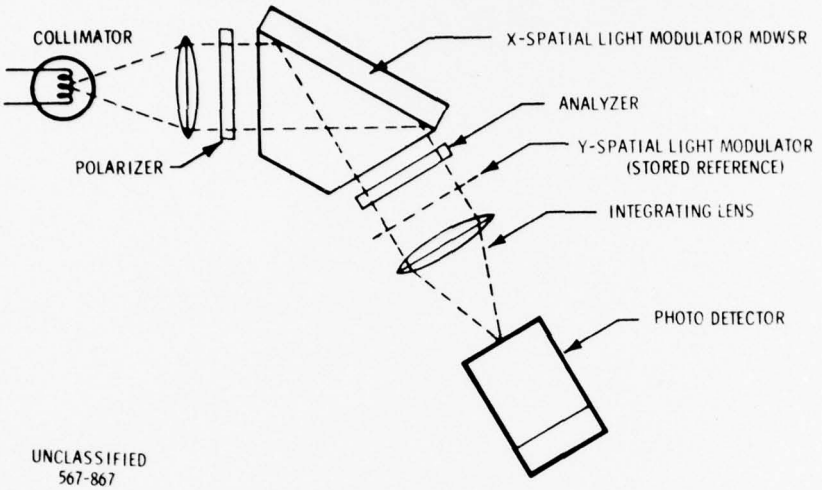

Figure 2-31 Non-Coherent Matched Filter Correlator Using a Magnetic Domain Wall Shift Register and Film as the X and Y Spatial Light Modulators

in the correlation function that are due to the DC light bias in each of the light modulators. While one of the error terms can be eliminated by AC coupling to the photodetector, the remaining error terms are generally random variables that are functions of the particular spatial X and Y patterns. These DC error terms can create significant problems of both scatter in the optics and saturation of the photomultiplier as well as contributing to the output noise, making it desirable to alter the DC component. In addition, the light source must be spectrally restricted to maximize the behavior of the X spatial light modulator. This in turn causes diffraction losses for a non-coherent configuration. The diffraction properties can best be used to actually control the DC components rather than be a source of loss. These benefits may be obtained from the coherent configuration illustrated in Figure 2-32. In this configuration appropriate transforming lenses and stops can control the DC components both in reduction of errors and for optimum adjustment of the percentage of modulation.

The first DC stop takes out the bias term from the first light modulator and thus removes two of the error terms inherent in the non-coherent correlator configuration. This occurs since the image of the first transforming lens is reflected Fourier transform of the spatial amplitude of the X light modulator. Hence the spatial frequency of the X signal is represented in the image plane where the DC stop is placed. This behavior is illustrated by viewing the image plane of the first transforming lens with a microscope. In Figure 2-33 a bench setup representing this portion of a "matched filter" correlator is illustrated. A 1/2-inch portion of a single track of the register is being used . A bit pattern of all ones is inserted, giving a 25 CPI square wave. Due to the propagation conductor spacing, a spectrum resulting from this input signal as viewed through the microscope is illustrated in Figure 2-34. The second transforming lens takes a Fourier transform of the signal which except for the reflection in scale factor is the inverse transform of the light intensity appearing in the first image plane, and places the reconstructed image on the surafce of the second light modulator where the X signal minus the error causing portion of the DC term is

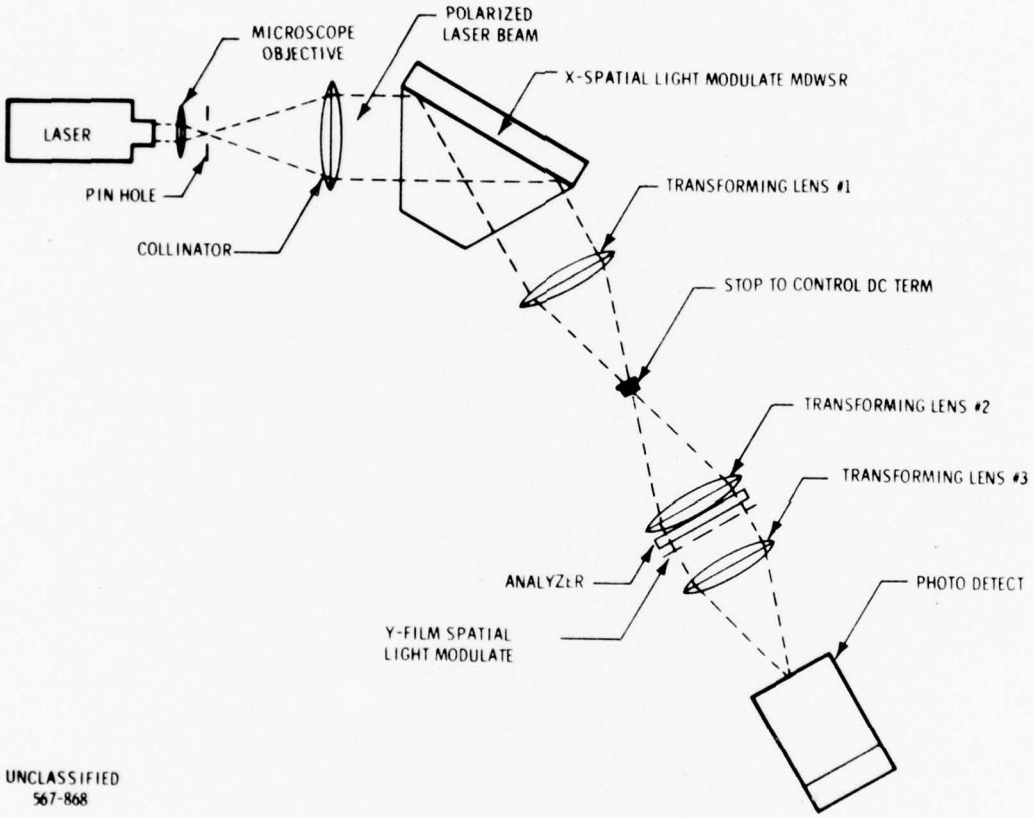

Figure 2-32. Coherent Matched Filter Correlator Using a Magnetic Domain Wall Shift Register and Film as the X and Y Spatial Light Modulators

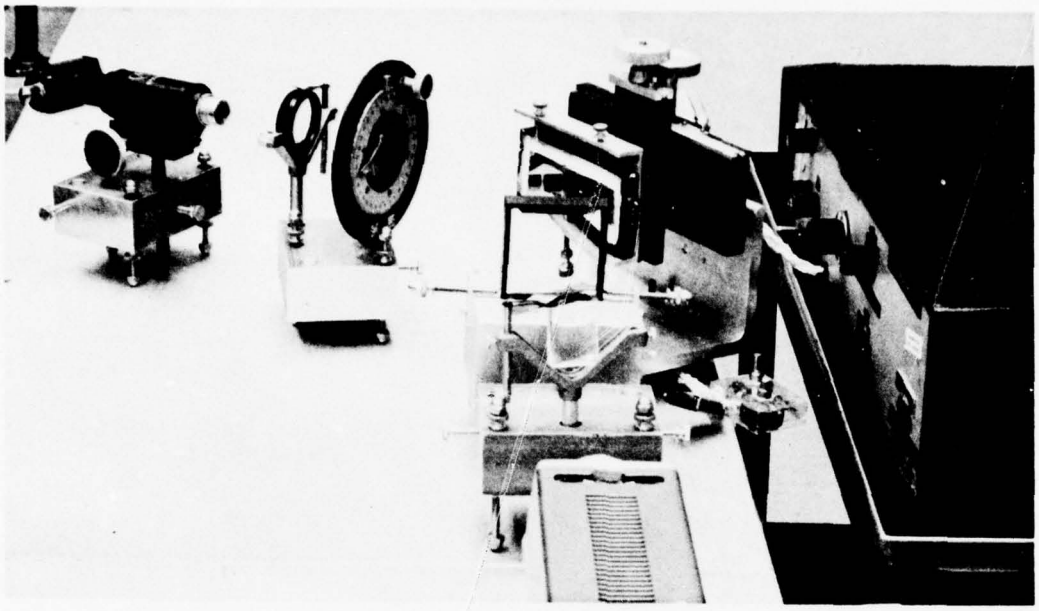

UNCLASSIFIED
567-869

Figure 2-33. Coherent Setup for the Magnetic Domain Wall Shift Register and First Transforming Lens

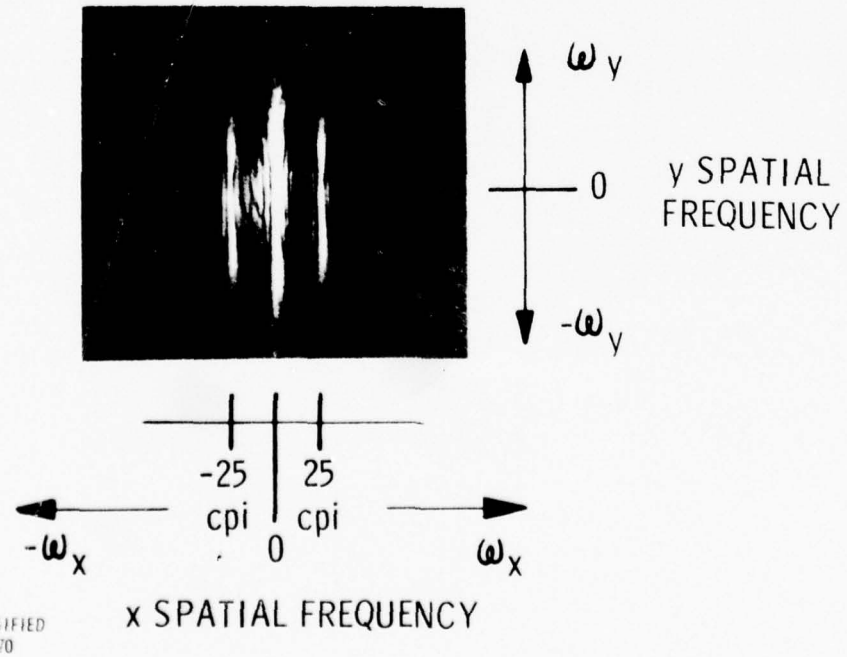

UNCLASSIFIED
567-870

Figure 2-34. Spatial Spectrum of Magnetic Domain Wall Shift Register as Viewed at Image Plane of First Transforming Lens

multiplied by the Y signal. Since no unmodulated light except that of the signal reaches the second modulator, two of the error terms are eliminated to the degree that the DC stop and other elements of the system approach the ideal. A second stop placed after the third transforming lens following the second or Y spatial light modulator would have the effect of removing the remaining error term; however, it is at this point in the image plane that the correlation term also appears. Thus, to separate the desired correlation signal from the DC error term, it is necessary to utilize a spatial carrier frequency with the Y pattern generator. However, this carrier is automatically introduced by the natural bit spacing in the magnetic domain wall shift register.

The bench setup for a complete "matched filer" correlator is illustrated in Figure 2-35. The output photodetector has a mechanical scanner for observing the full image plane. This allows viewing of the correlation function at the sideband location and provides a convenient means of observing the effects of simulated doppler, etc. This scanner may be replaced by a solid state scanning array of the type that has been recently developed for compact video and IR scanning applications.

In a time-varying correlator, both the X and Y spatial light modulators accept time varying signals. Such a configuration with a coherent light source is illustrated in Figure 2-36. This configuration is essentially the same as the "matched filter" configuration of Figure 2-32 except that the film spatial light modulator has been replaced by a magnetic domain will shift register spatial light modulator. A bench setup of this configuration is illustrated in Figure 2-37. It should be noted that the operation of this configuration also includes the "matched filter"mode since any pattern shifting through the Y spatial light modulator may be stopped and is equivalent to a piece of film except for the insertion loss.

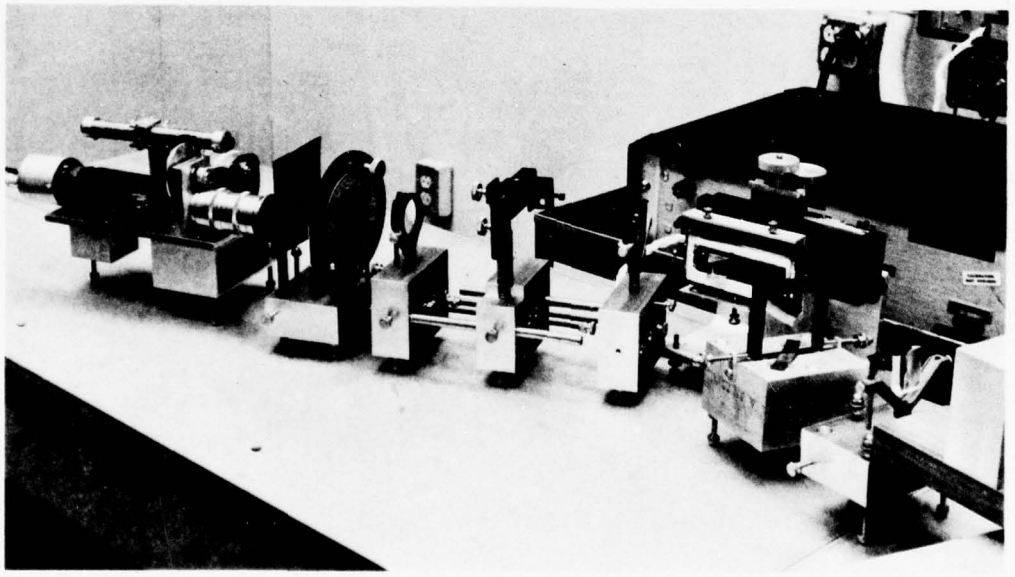

UNCLASSIFIED
567-880

Figure 2-35. Bench Setup for a Coherent Matched Filter Correlator Using a Magnetic Domain Wall Shift Register and Film for the X and Y Spatial Light Modulators

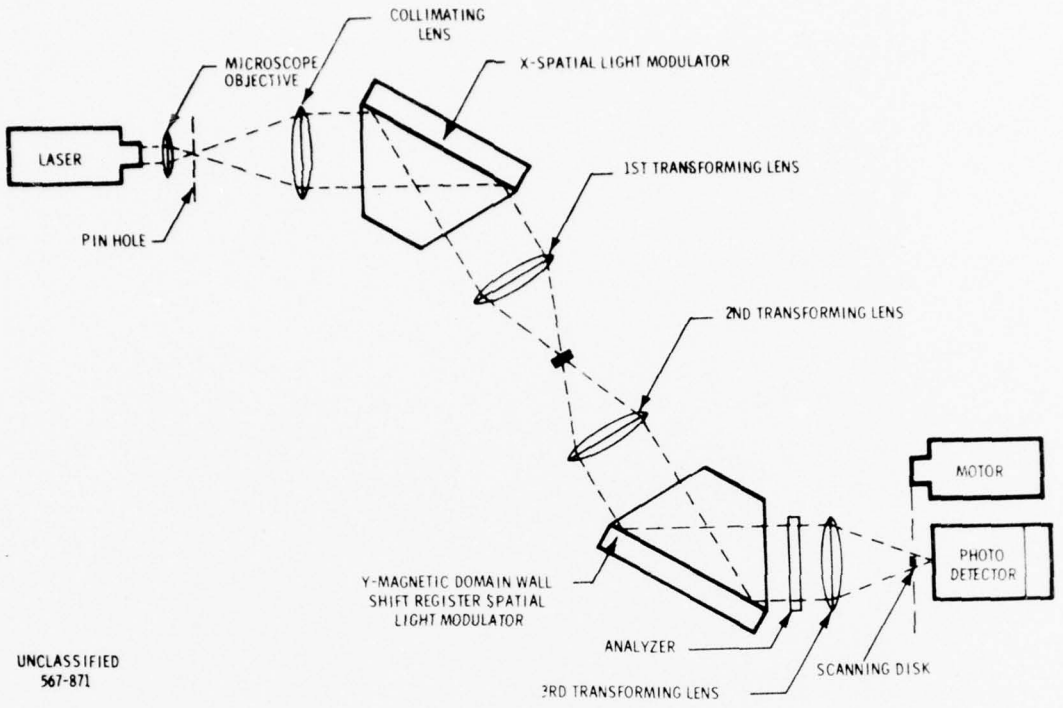

Figure 2-36. Time-Varying Coherent Correlator Configuration

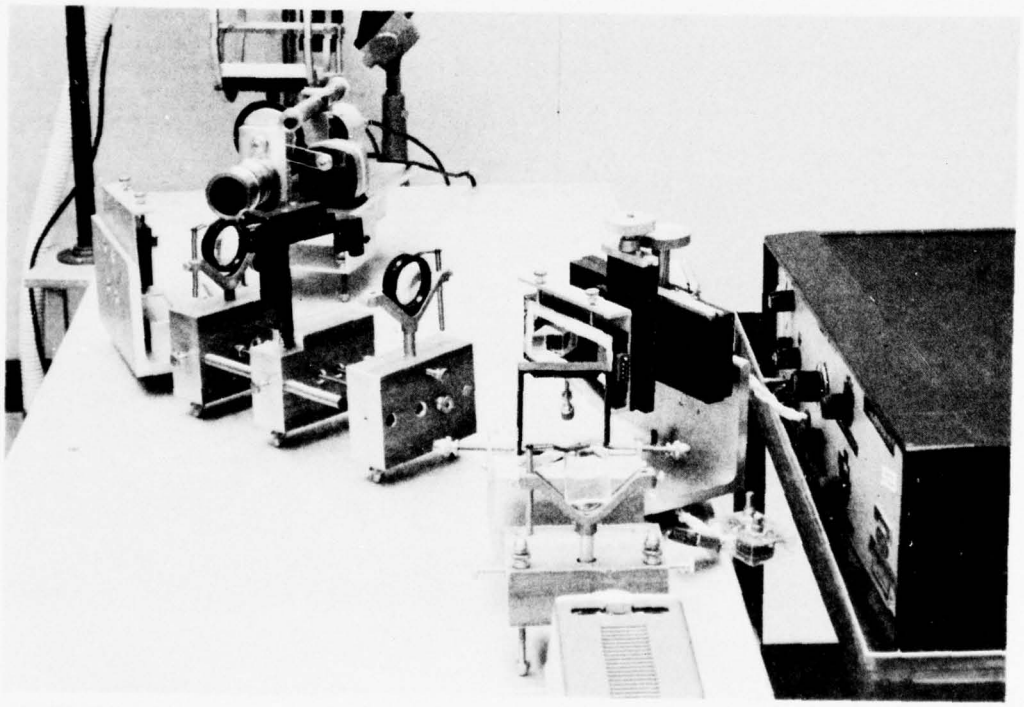

UNCLASSIFIED
567-872

Figure 2-37. Bench Setup, Time-Varying Coherent Correlator Using Magnetic Domain Wall Shift Registers as the X and Y Spatial Light Modulators

A conceptual drawing of a time varying correlator configuration indicating the relative size of a unit employing all solid state components is illustrated in Figure 2-38.

An interesting use of a spectrum analyzer configuration in reducing the search time for narrowband information modulated on a wideband complex carrier is illustrated in Figure 2-39 and 2-40. Here the analyzer determines the frequency uncertainty in the modulator load time, thus eliminating the need for a separate frequency search at each code clock interval.

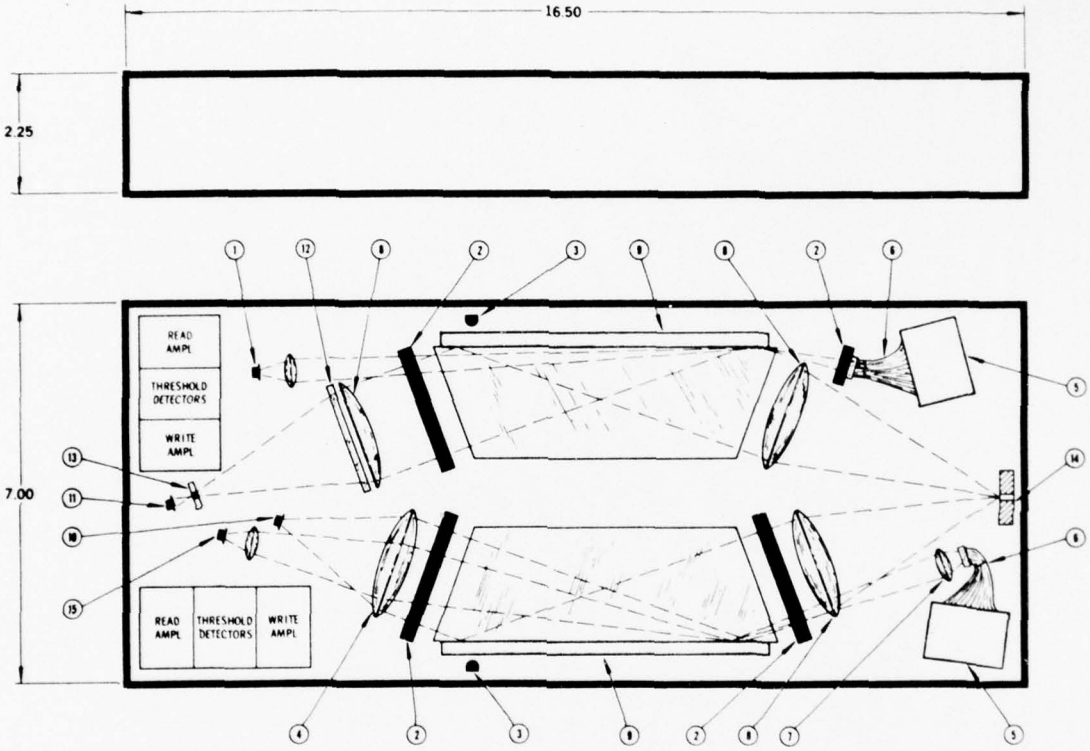

Figure 2-38. Conceptual Drawing of a Magneto-Optic Correlator Utilizing Solid State Components

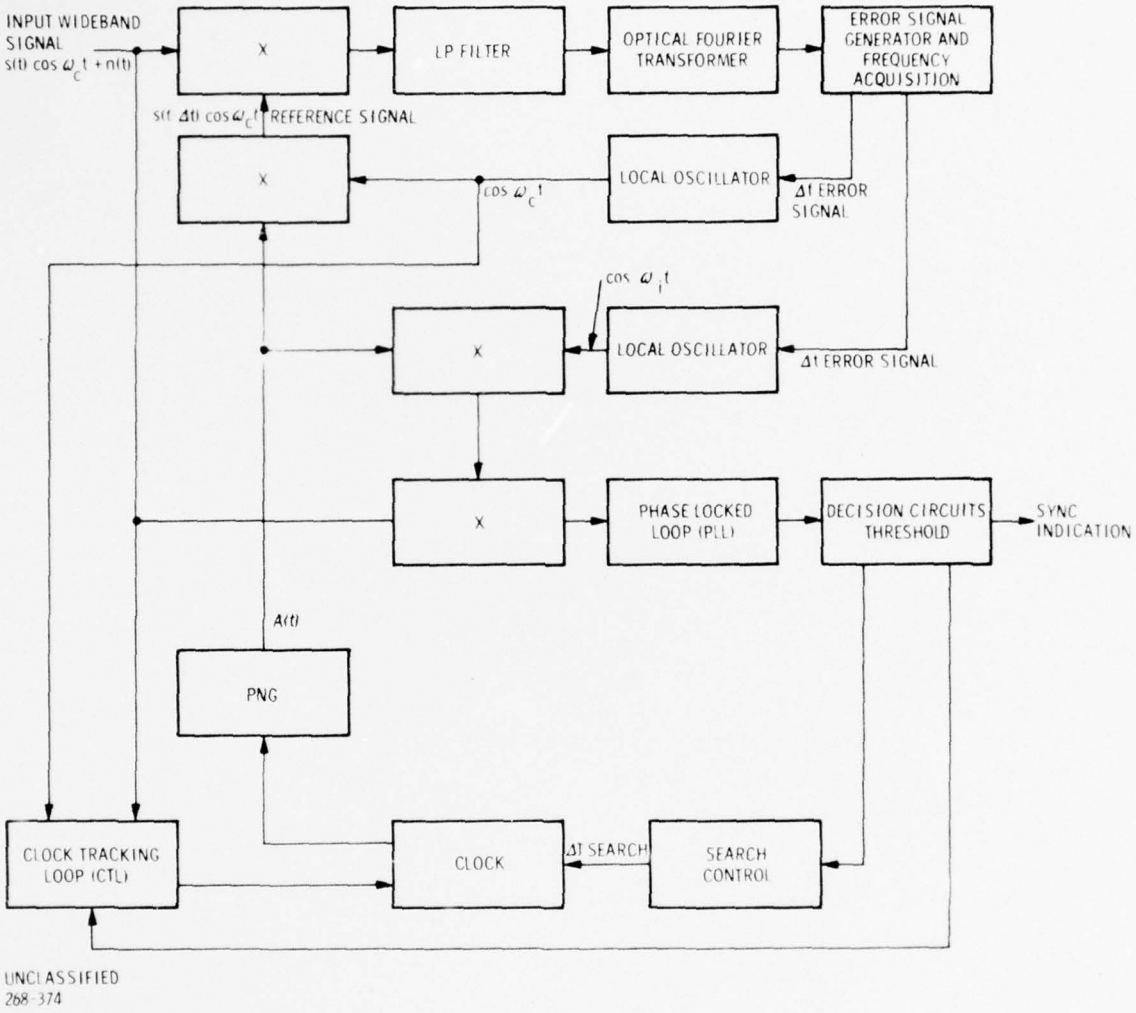

Figure 2-39. Classical Sliding Correlator Synchronizer Augmented by Optical Fourier Transformer to Eliminate the Frequency Search

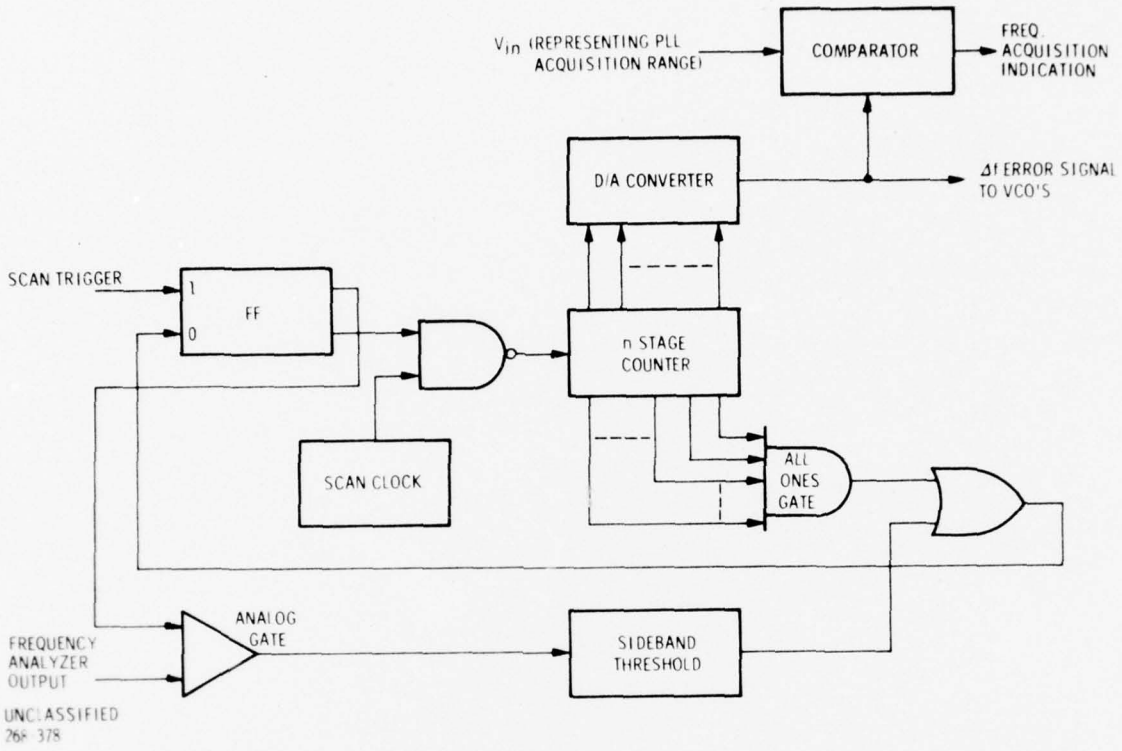

Figure 2-40. Functional Diagram of Error Signal Generation and Frequency Acquisition Indication

REFERENCES

1. Peter Elias, "Optics and Communication Theory," J. Opt. Soc. Am., 43, No. 4, 229-232 (Apr 1953)

2. Peter Elias, David S. Grey, and David Z. Robinson, "Fourier Treatment of Optical Processes," J. Opt. Soc. Am., 42, No. 2, 127-134 (Feb 1952)

3. L.J. Cutrona, E.N. Leith, C.J. Palermo, and L.J. Procello, "Optical Data Processing and Filtering Systems," IRE Trans. on Information Theory, IT-6, No. 3, 386-400 (Jun 1960).

4. Kendall Preston, Jr., "Computing at the Speed of Light," Electronics, 72-83 (6 Sept. 1965)

5. R.E. Eschelbach, "A General-Purpose Multichannel Coherent Processer Using the Kerr Magneto-Optic Effect for Electrical Signals Linearly Recorded on Magnetic Tape," MRL Rpt. No. R-1383 (1 Nov 1966).

6. Victor C. Anderson, "Digital Array Phasing," J. Acous. Soc., Am., 32, No. 7, 867-870 (Jul 1960)

7. Philip Rudnick, "Small Signal Detection in the DIMUS Array," J. Acous. Soc. Am., 32, No. 7, 871-877 (Jul 1960)

8. A Mickael Noll, "Short-Time Spectrum and "Cepstrum" Techniques for Vocal-Pitch Detection," J. Acous. Soc. Am., 36, No. 2, 296-302 (Feb 1964)

9. R.E. Eschelbach, "Multi-Mode Radar Clutter Processer - Phase I Report, "MRL Rpt. No. 1642 (25 Jan 1968)

10. L.J. Cutrona, W.E. Vivian, E.N. Leith, and G.O. Hall, "A High-Resolution Radar Combat-Surveillance System," IRE Trans. on Military Electronics, MIL-5, No. 2, 127-131 (Apr 1961)

11. L. J. Cutrona, E.N. Leith, L.J. Porcello, and W.E. Vivian, "One the Application of Coherent Optical Processing Techniques to Synthetic-Aperture Radar," Proc. IEEE, 54, No. 8, 1026-1032 (Aug 1966)

12. R. E. Eschelbach, "Scale Factor for the Fourier Transform of a Spatial Light Modulat or with a Titled Signal Plane," MRL Tech. Memo. (Feb 1968)

13. R. E. Eschelbach, "Non-Coherent and Coherent Optical Correlators Using the Kerr Magneto-Optic Effect for Real-Time Electrical Signals," MRL Rpt. No. R-1418 (30 Dec 1966)

14. R.E. Eschelbach, "Optical Techniques in the Synchronization of Pseudonoise Communication Systems," MRL Tech. Rpt. No. MX-TR-8-690-2004-68 (1 Mar 1968)

APPENDIX A

SPATIAL LIGHT MODULATION WITH THE KERR MAGNETO-OPTIC EFFECT

APPENDIX A

SPATIAL LIGHT MODULATION WITH THE KERR MAGNETO-OPTIC EFFECT

The Kerr magneto-optic effect is a change of either rotation or reflection of incident polarized light on a ferromagnetic surface by the magnetic state of the surface. The particular effect that has received the majority of attention at Magnavox Research Laboratories is the longitudinal Kerr effect in which the magnetization is parallel to the plane of incidence of the polarized light as illustrated in Figure A-1. The reason for this emphasis is two-fold. By using the longitudinal Kerr effect, the percentage of modulation may be adjusted at the expense of insertion loss. Thus contrast ratios approaching 100% may be obtained. A second advantage of the longitudinal effect is that the DC term may be extinguished to an extent that it is a function only of the quality of the polarizing elements utilized. This is particularly important in coherent processing applications where the quality of the output image may be seriously degraded by optical bulk and surface scatter. Reducing the DC term minimizes the effects of scatter and eliminates the need for spatial filtering of the DC term in the frequency domain. This latter mode of operation is possible since it is the polarization discontinuities that are the source of diffraction in the plane of the spatial light modulator rather than the observable changes in intensity existing at the second polarizer or analyzer in the system. Other magneto-optic effects that can be considered with some advantage are the polar and transverse Kerr effects as well as the Faraday effect. The Faraday effect covers a change in rotation or transmission as the light passes through the material and is of the same generic form as the various Kerr effects except that they involve the reflection rather than the transmission of light.

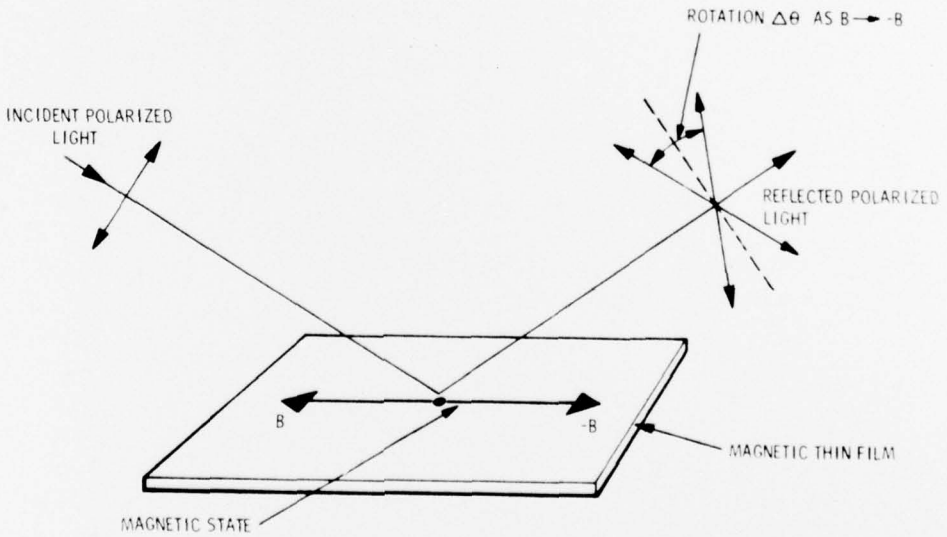

Figure A-1. Kerr Longitudinal Magneto-Optic Effect

A basic spatial light modulator utilizing the longitudinal Kerr magneto-optic effect is illustrated in Figure A-2. The incoming light is polarized in the plane of incidence by a polarizer (or a polarized light source such as a gas laser may be used). A prism is utilized to provide a rigid substrate and to efficiently couple the polarized light to the thin film. A magnetic pattern generator in conjunction with the thin film

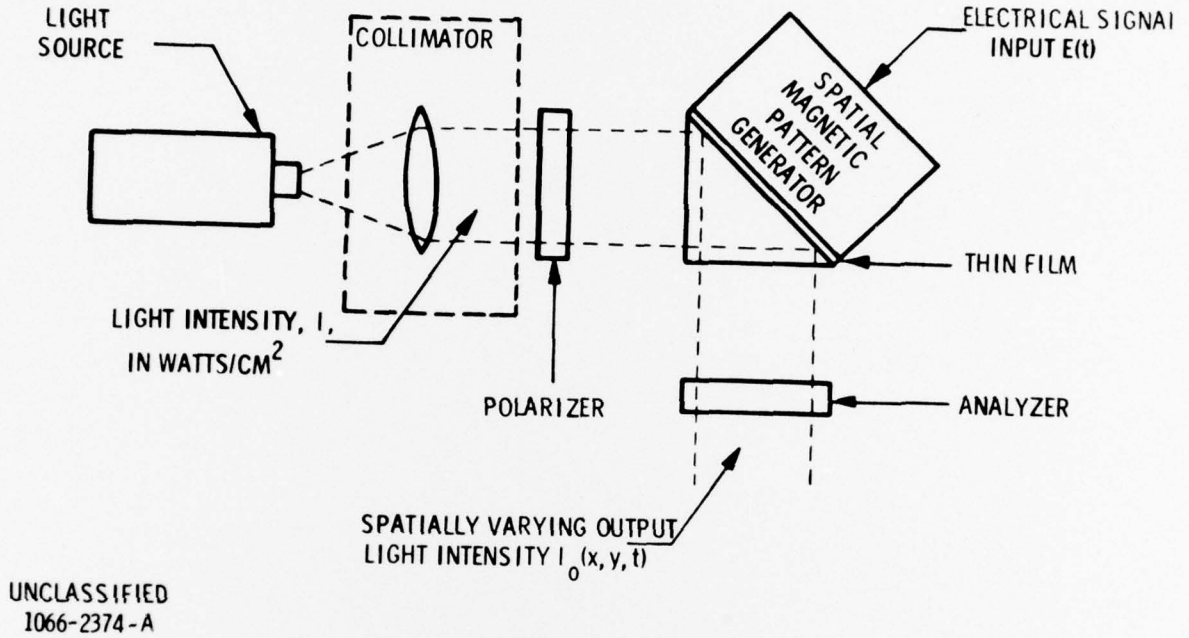

Figure A-2. Basic Spatial Light Modulator Using Longitudinal Kerr Magneto-Optic Effect

spatially changes the magnetic state of the thin film. A second polarizer placed as an analyzer in the light path from the prism serves to convert the changes of rotation experienced at the surface either to a change in intensity, if direct viewing is of interest, or to eliminate the DC term, when coherent processing of the information is desired. This intensity-rotation interchange depends on an analyzer-polarizer operation curve as illustrated in Figure A-3. Here the quiescent operating point is determined by the rotation of the analyzer relative to the polarizer referenced to the extinction point.

An important consideration is the orientation of the anisotrophy axis of the film to the plane of incidence. For the easy magnetic axis of the film oriented parallel to the plane of incidence, the induced field can have essentially only two values, B_S and $-B_S$, giving only two rotations, $\pm \frac{\Delta\theta}{2}$ and has only two intensity values from the polarizer-analyzer operating curve.[2] In this mode, the thin film exhibits memory, so that if the pattern generator is removed the pattern will remain. This property is of value for stationary or quasi-stationary "matched filtering" operations such as encountered in correlation or in any case where it is desired to have a non-vortal storage of the information to be processed. However, in this mode of operation the light modulator has the defect of behaving as an ideal symmetric hard limiter. In this mode of operation the limiting action can cause processing losses as high as

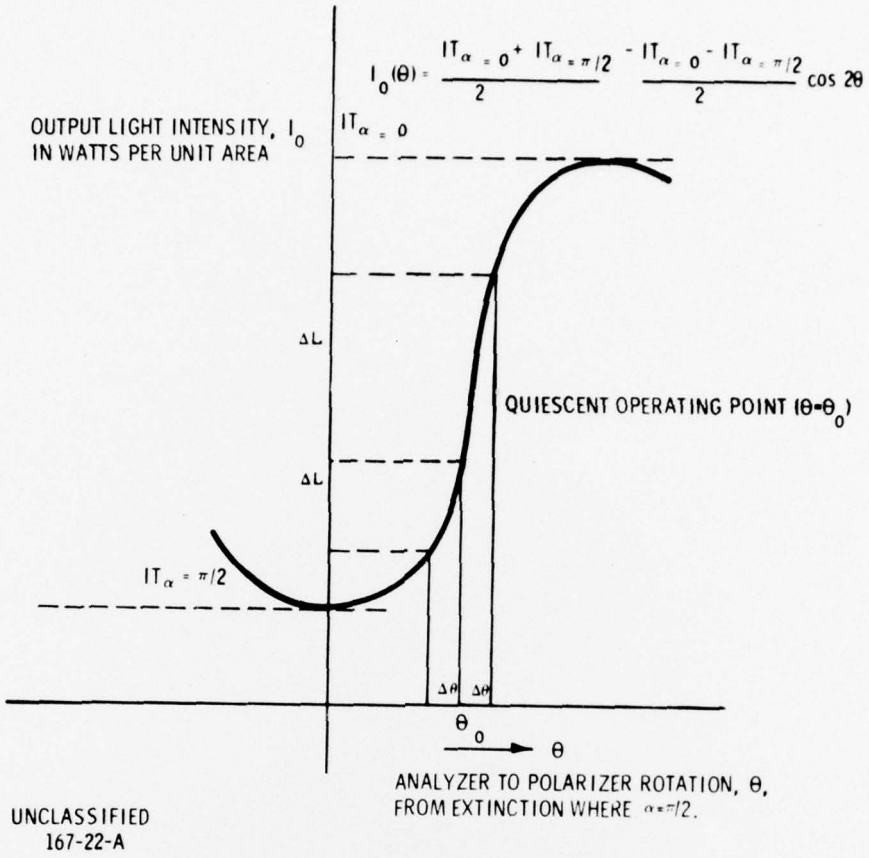

Figure A-3. Modulator Operating Curve

6 DB for constant envelope interference (references A1 and A2). However, for noise interference, the loss due to the limiting action is only 1 DB or so. While hard limiting behavior is allowable for a variety of signal processing techniques, the limiting action can be avoided with a hard magnetic axis orientation of the thin film. For this orientation, the induced field and hence Kerr rotation is linearily proportional to the inducing field H until a value of $\pm H_K$, the anisotrophy field is reached. Since there is no remanence in the hard axis orientation, the necessity for a bias field to erase the thin film as the pattern is changed is also removed and linearity and Gray scale result for both imaging and processing applications. The B - H curves of ideal easy and hard axis thin film orientations are shown in Figure A-4, while typical values obtained from a Kerr B-H Tester and illustrated in Figure A-5. A typical curve illustrating the linearity flux leakage coupling into the thin film is illustrated in Figure A-6.

A1. C. R. Cahn, "Note on Signal-to-Noise Ratio in Bandpass Limiters," IRE Trans. on Information Theory, IT-7, No. 1, 39-43 (Jan 1961)

A2. R. E. Eschelbach, "The Effect of Hard Limiting in Satellite Repeaters on Signals Employing Angle Modulation," Reprinted from Ballistic Missile and Space Technology, I, 241-293 Academic Press In. c, (1960)

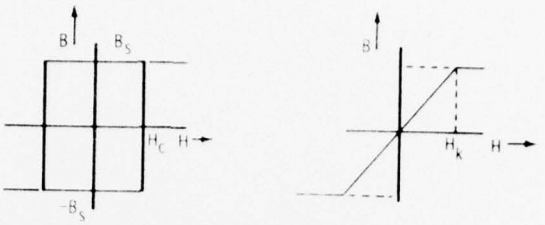

UNCLASSIFIED
966-1793

Figure A-4. Ideal B-H Curves of Easy and Hard Oriented Magnetic Thin Films

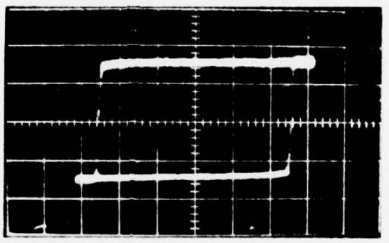

EASY AXIS OF THIN FILM 656 H_C = 25 OERSTEADS

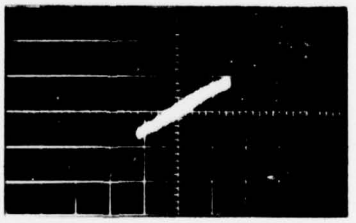

HARD AXIS OF THIN FILM 674CJ HLH$_K$: H_K = 26 OERSTEADS

UNCLASSIFIED
1167-2422

Figure A-5. Typical B-H Curves of Easy and Hard Oriented Magnetic Thin Films Obtained by Magneto -Optic Readout

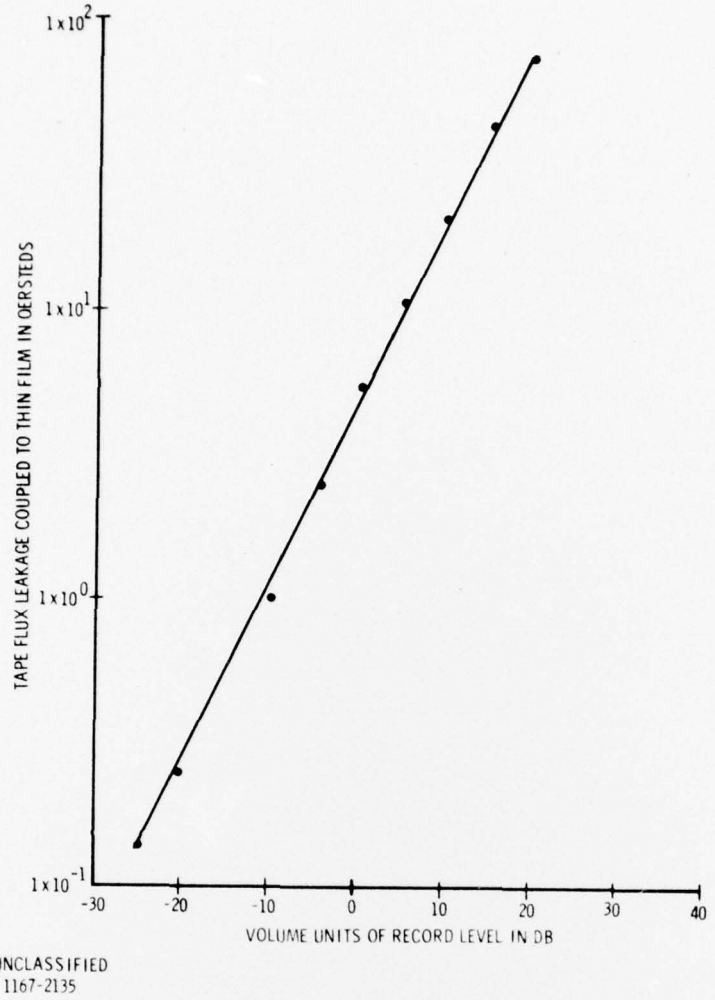

Figure A-6. Flux Leakage into Magnetic Thin Film from Recording Tape with One Mill Mylar Spacing as a Function of Record Level

The simplest case of a magnetic pattern generator is a piece of linearily recorded magnetic tape placed against an appropriate thin film structure. Here the flux leakage from the tape causes a change in rotation or reflectance that is a function of the chosen quiescent operating point, the amount of flux leakage, and the thin film orientation as introduced above. With such a spatial light modulator, linear densities in the order of 2,000 bits per inch with bandwidths up to 200 MHz have been successfully read by magneto-optic techniques (references A3 and A4) where a magnetically saturated

A3. J.J. Miyata and T. Lentz, "MAGOP - A New Approach to High-Density Magnetic Recording," Presented at Symposium on Large Capacity Memory Techniques for Computing Systems (May 1961)

A4. D.A. Thompson, and H. Change, "Nanosecond Microscopic Measurement of Magnetic Film Switching b Kerr Magneto-Optic Apparatus. Phys. Stat. Sol., 17, No. 83, 83-90 (1966)

recording medium has moved under a spot of light in a Kerr magneto-optic structure. At Magnavox Research Laboratories, Kerr readouts exhibiting packing densities in excess of 10,000 CPI have been obtained. An area readout from a light modulator of the type illustrated in Figure A-1 is illustrated in Figure A-7. The information in this case was recorded on tape with a transverse recording head at a density of 1,000 bits per inch in the direction of head movement and at a density of 100 channels per inch in the direction of tape movement.

As previously indicated, modulators utilizing the longitudinal Kerr effect may allow adjustment of the percentage of modulation to optimize contrast ratio if viewing is of interest, or control the amount of DC light appearing in the output without spatial filtering if signal processing is of interest. This behavior may be seen by referring to the polarizer-analyzer operating curve. Thus, near extinction, where the operating

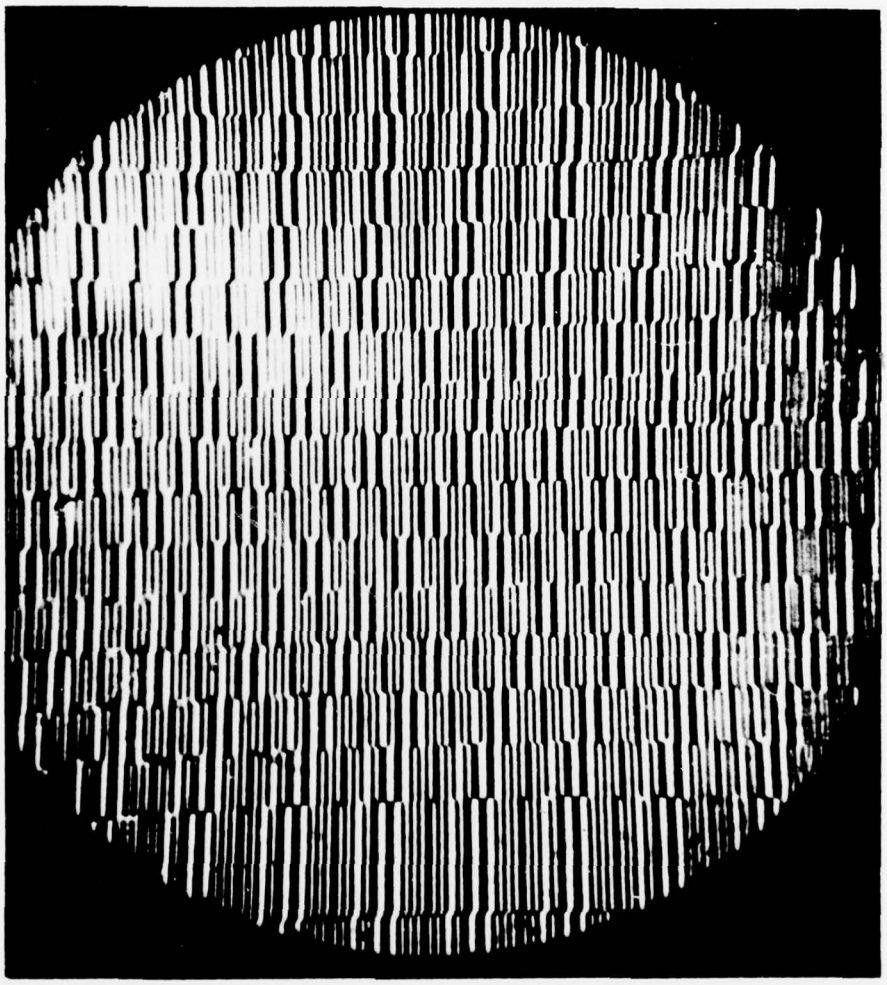

UNCLASSIFIED
1065-1306-A

Figure A-7. Magneto-Optic Area Readout of Magnetic Tape Pattern Generator With a Packing Density of 1,000 Bits Per Inch by 100 Bits (Tracked Per Inch)

point $\theta_o = \frac{\Delta\theta}{2}$, the light output, $I_o(\theta', \theta_o)$, as a function of the spatial modulating function $\theta'(x, y, t)$ is given by

$$I_o = \frac{I(T_o + T\pi/2)}{2} - \frac{I(T_o - T\pi/2)}{2}(\cos 2\theta_o \cos 2\theta' - \sin 2\theta_o \sin 2\theta')$$

but the percent modulation, M, for $\Delta\theta \ll 1$ is given by

$$M = \frac{\Delta I_o(\theta)}{I_o} \approx \frac{T_o \theta^2}{T\pi/2} \quad \text{since } \cos 2\theta' \approx 1 - \theta'^2$$

Hence, M is inversely proportional to the insertion loss $\frac{T_{\pi/2}}{T_o}$ in the vicinity of $\theta_o = 0$ and is proportional to the square of achievable rotation, θ'. At $\theta_o = 0$, $\Delta I(\theta') = 0$ but both polarization and phase changes allow efficient spatial modulation of the incident light.

While the use of tape as a transfer pattern generator as described above is desirable for a large variety of imaging and signal processing problems and is competitive in optical processing applications requiring information densities approaching those achievable from film, it is desirable to consider other magnetic storage techniques with spatial transfer in which the mechanical movement of the storage medium as used with the tape technique illustrated above has been excluded. This leaves consideration of techniques such as:

- Magnetostrictive variation of a magnetic field in a linear medium
- Thermomagnetic modification of the medium
- Magnetic core or aperture plates storage transfer movement
- Thin-film storage and transfer
- Magnetic domain wall movement as a linear shift register

The first technique suffers from the same problem as the Sears-Debye effect, namely relatively high propagation velocities which result in a low information packing density. In addition, magnetostrictive transducers generally have much lower available bandwidths and efficiencies then the piezo electric transducers utilized with quartz delay lines (e.g., the bandwidth is usually less than 1 MHz and insertion losses in the order of 80 DB or higher may be encountered at these bandwidths). However, acoustic and electromagnetic interractions at much higher frequencies have been reported in the literature and the possibility of considering multiple thin film channels appears to offer significant advantages over similar techniques utilizing the Sears-Debye effect.

The second category of techniques involving the thermomagnetic modification of a magnetic medium is under continuing investigation and will not be reported at this time. For certain applications, such as those involving the correlation of wideband signals, one drawback does occur in the application of this technique since an erasure is required after each frame is written in order to move the information to the next position although writing rates consistent with the large signal bandwidths is possible for each frame. To achieve a shift register type of operation in which the pattern moves continuously within the frame or aperture will require a different form of operation than is currently envisioned.

Initial efforts in dynamic magnetic pattern generation have involved the utilization of magnetic cores potted in an array and ground flat so as to allow flux leakage onto the thin film. The primary problem with the use of cores centers upon the transfer of information in one core to another for a shift register type of operation in the pattern generator. If such shift registers are to be operated at the maximum switching rate of the cores, then the amount of drive circuitry needed for the transfer tends to increase since only partial switching results at switching rates in the order of 10 MHz or greater. At lower rates all magnetic shift register structures are possible, but still exhibit problems in regard to packing density due to the size of the multiple aperture core structures required.

While similar comments apply to the utilization of thin film techniques as storage media, recent results indicate that with appropriately deposited strip line structures the state of the thin film may be switched with reatively low drive currents (e.g., in the order of 35 milliamperes or less). There is some indication that even lower drive currents may be possible. This will allow consideration of hybrid solid state transfer structures mounted directly on the thin film memory. Therefore, consideration for further effort is being given to this approach.

The most immediate solution, however, appears to be the utilization of shifting techniques involving the movement of domain walls within the thin film medium itself. For this reason the major portion of the effort to date has centered upon magnetic domain shift wall registers. This emphasis is warranted because of both the proven operation of the register and the packing densities and information rates obtainable. Spatial light modulators utilizing this approach are discussed in the following section.

APPENDIX B

MAGNETIC DOMAIN WALL SHIFT REGISTER (MDWSR) SPATIAL LIGHT MODULATORS

APPENDIX B

MAGNETIC DOMAIN WALL SHIFT REGISTER (MDWSR) SPATIAL LIGHT MODULATORS

Thin film magnetic domain wall shift registers were first described in reference B1. The shift registers currently under development are proprietary improvements of this basic configuration. To explain the operation of this device, consider a magnetic thin film deposited in a long, narrow channel as illustrated in Figure B-1. Consider that the channel or thin film strip is initially biased in a given magnetic direction representing, for example, all zeroes. The write head then reverses the field direction causing a one to appear in the immediate vicinity of the write head. Under a Kerr magneto-optic readout structure, the one would appear dark while the zeroes along the remaining portion of the channel would appear light. Appropriate current conductors or strip lines placed adjacent to the thin film channels can shift the information up or down the channel depending upon the phase of the currents in the propagation conductors. In this sense, the shift register acts as the equivalent to a piece of magnetic tape that would be moving past the optical aperture, in fact there is only movement of the magnetic domain walls since the structure is stationary. The information is propagated along the continuous thin film strip by translating the domain walls in such a manner as to preserve their essential domain configuration. Thus, the associated electronics for the shift register consist of solid state write drivers for each channel, a clock generator, and two current drivers, giving the four phase current waveforms shown in Figure B-2.

A shift register structure on a glass substrate is illustrated in Figure B-3. A typical bit pattern on a portion of three channels on a 12-channel register is illustrated in Figure B-4 by means of a visual Kerr readout. The optical readout of the information in a given channel of the shift register may also be accomplished by focusing polarized light onto the desired portion of the channel. In addition, an analyzer lens and photo-multiplier are coupled to the shift register as illustrated in Figure B-5. A typical electrical input and its optical readout down the channel is illustrated in Figure B-6.

A convenient feature of the shift register is its nonvolatile storage of information and the ability to shift the information in either direction. Whenever the propagate current waveforms are inhibited, the information contained in the register remains until the propagate pulses are reactivated, thus providing nonvolatile storage of the information. Currently achievable information densities are in the order of 62 bits to the inch per channel with channel densities of 100 channels to the inch. This latter density is constrained primarily by the achievable size of the write heads and not by the thin film properties of the register. Thus storage densities in the order of 6000 bits per square inch are achievable with this nonmoving part type of spatial light modulator. Such a modulator finds its major uses in correlation structures involving moderate numbers of bits (as for example, in pattern recognition problems where large TW products are not a requirement or in beam-forming applications involving moderate numbers array elements where each element serves as an output to the separate tracks of the register). For higher densities, the use of either tape or thermomagnetic modulation techniques is indicated. While magnetic domain wall shift register modulators do not have sufficient packing density to make them usable as high-resolution spectrum analyzers, the packing densities are sufficient to allow separation of the signal and DC terms by coherent operation of the

B1. Kent D. Broadbent, "A Thin Magnetic Film Shift Register," IRE Trans. on Elect. Comp., Sept. 1960.

correlator. For example, consider the signal obtained in the Fourier transform plane from such a modulator with a packing density of 25 bits per inch as illustrated in Figure B-7. Here elimination of the DC term will aid in the removal of error terms in processing structures involving, for example, correlation.

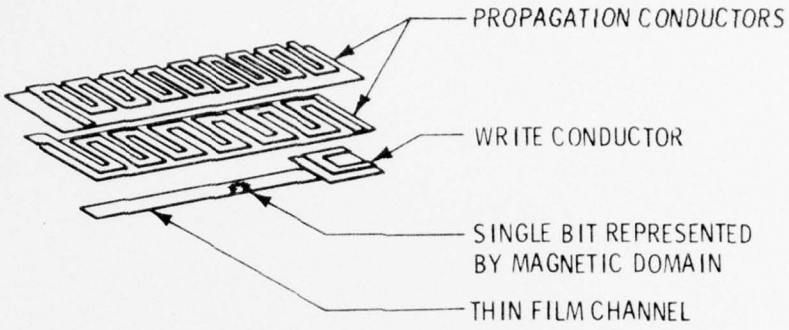

Figure B-1. Thin Film Shift Register Structure

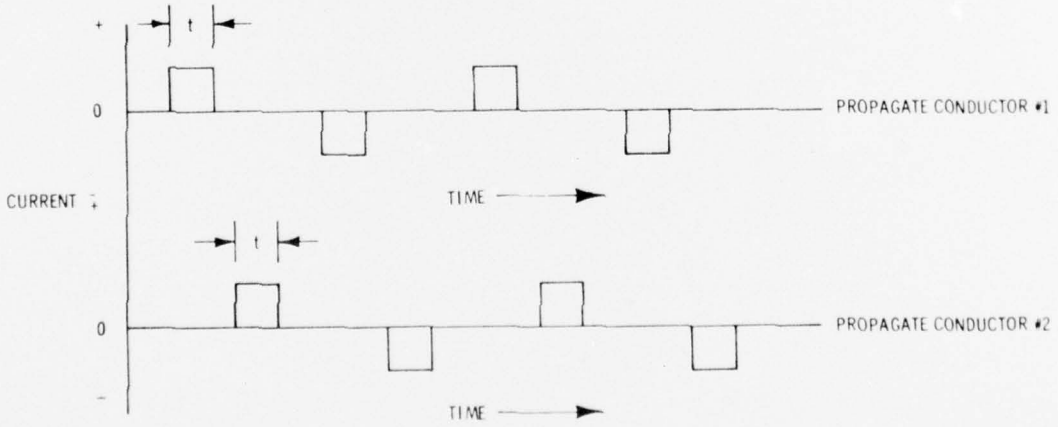

Figure B-2. Propagate Current Waveforms

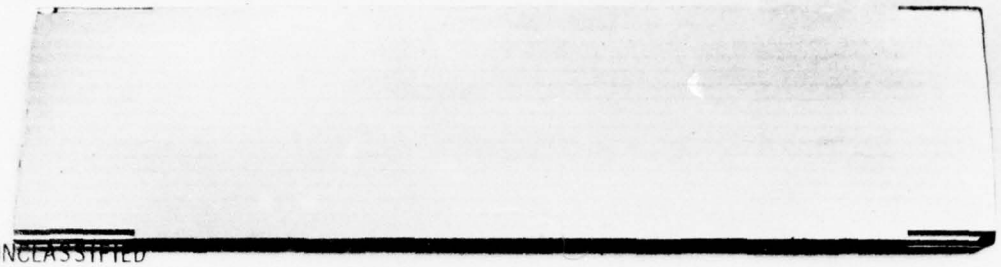

UNCLASSIFIED
567-865

Figure B-3. Magnetic Domain Wall Shift Register on a Glass Substrate

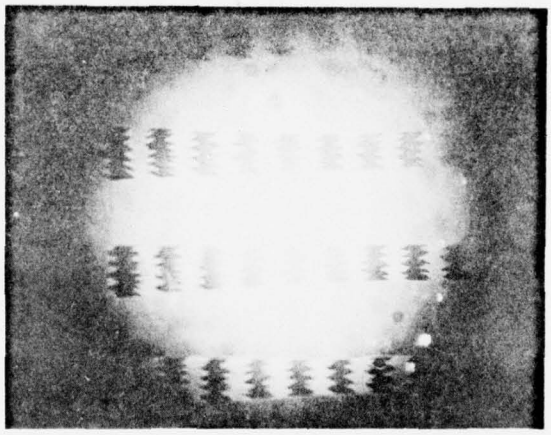

UNCLASSIFIED
567-866

Figure B-4. Visual Readout of a Portion of 3-Channel of a 12-Channel MDWSR With A 101010 . . . . Pattern on Each Channel

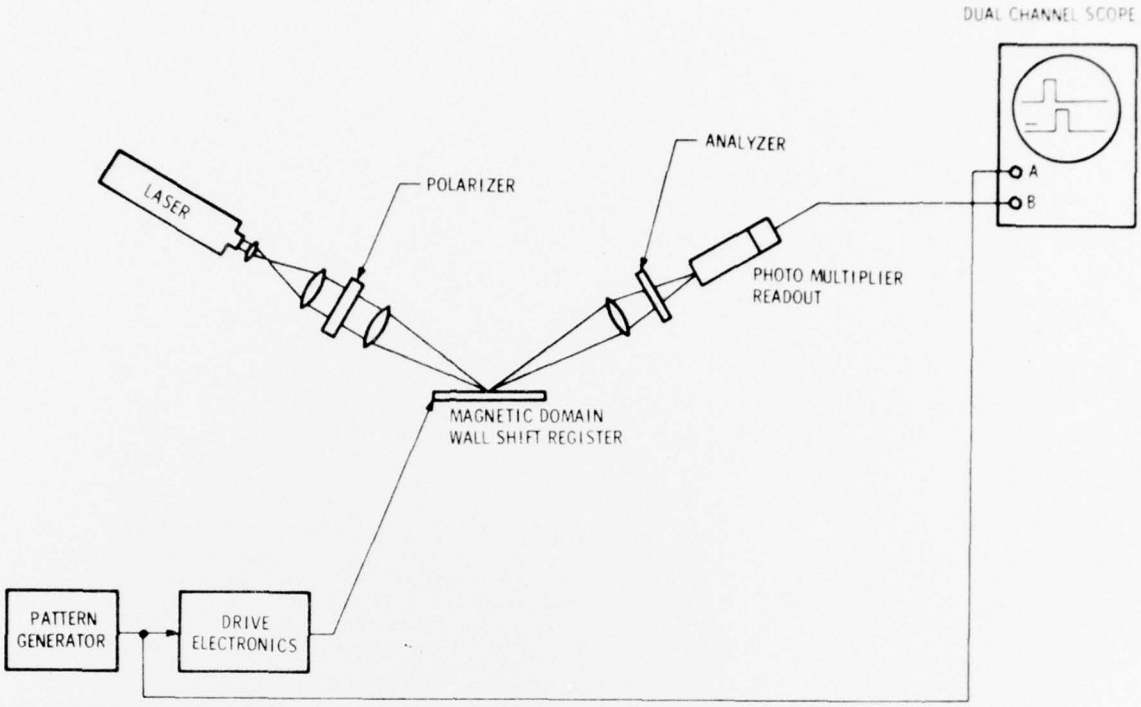

Figure B-5. Test Setup For Optical Readout of Magnetic Domain Wall Shift Register

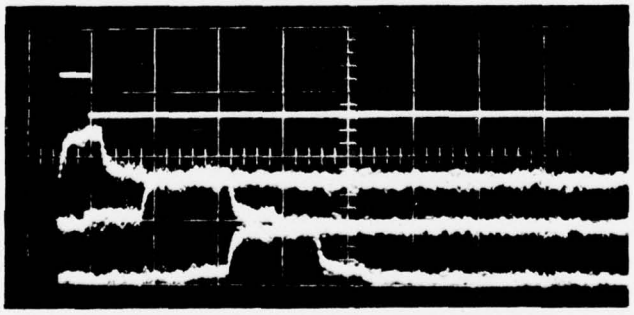

TRACE 1: INPUT DATA WRITE CURRENT FOR 1000 PATTERNS 1 AM/CM

TRACE 2: OPTICAL READOUT OF WRITE CURRENT

TRACE 3: OPTICAL READOUT AT X_1 INCHES FROM DATA ENTRY.

TRACE 4: OPTICAL READOUT AT X_2 INCHES FROM DATA ENTRY

HORIZONTAL: 200 μs/CM

UNCLASSIFIED
368-550

Figure B-6. Input and Output Data Waveforms for Signal Channel Shift Register Test Set

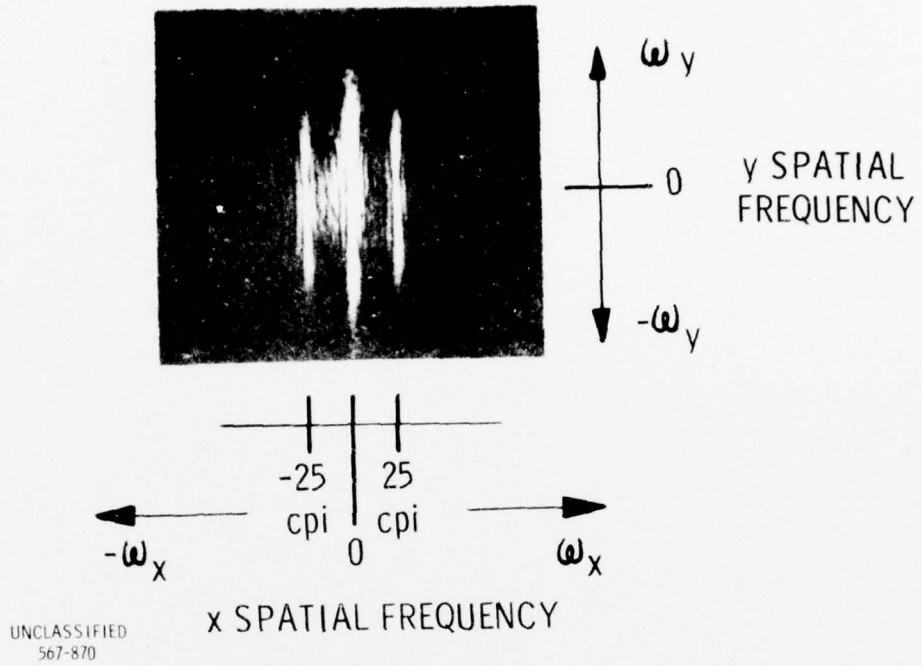

Figure B-7. Spatial Spectrum of Magnetic Domain Wall Shift Register as Viewed at Transform Plane


DAT
ILM